High-Temperature Vaporization Behavior of Oxides II. Oxides of Be, Mg, Ca, Sr, Ba, B, Al, Ga, In, Tl, Si, Ge, Sn, Pb, Zn, Cd and Hg

R. H Lamoreaux and D. L. Hildenbrand

SRI International, Menlo Park, California 94025

and
L. Brewer

Department of Chemistry, University of California, Berkeley, California 94720

Received December 8, 1983; revised manuscript received November 28, 1986

In order to assess the high-temperature vaporization behavior and equilibrium gas phase compositions over the condensed oxides of Be, Mg, Ca, Sr, Ba, B, Al, Ga, In, Tl, Si, Ge, Sn, Pb, Zn, Cd, and Hg, the relevant thermodynamic and molecular constant data have been compiled and critically evaluated. Selected values of the Gibbs energy functions of condensed and vapor phases are given in the form of equations valid over wide temperature ranges, along with the standard entropies and enthalpies of formation. These data were used to generate plots of equilibrium partial pressures of vapor species as functions of temperature for representative environmental conditions ranging from reducing to oxidizing. The calculated partial pressures and compositions agree, for the most part, with experimental results obtained under comparable conditions. Maximum vaporization rates have been calculated using the Hertz–Knudsen equation. Literature references are given.

Key words: critically reviewed data; enthalpy increment; enthalpy of formation; entropy; Gibbs energy function; high temperature; oxide; partial pressure; thermodynamic data; vaporization; vaporization rate.

Contents

List of Tables

List of Figures

1. Introduction

1.1. Background

Oxide materials are used or encountered in a wide variety of high-temperature applications where vaporization rates and thermodynamic stabilities are often limiting factors. The efficient design and operation of high-temperature devices and processes requires reliable information about the stability and volatility of these oxides so that vaporization losses and component lifetimes can be predicted.

Despite continuing research efforts and the use of increasingly sophisticated techniques, there are still many gaps in our knowledge and understanding of the detailed vaporization thermodynamics of metal oxide systems. This puts a premium on critical review of the literature and selection of the necessary thermodynamic data. However, even in cases where most of the requisite data are compiled, the user must resort to a significant amount of additional calculations, sometimes unfamiliar, in order to evaluate vapor composition and vaporization behavior for specific environmental conditions. Thus we perceive a definite need for critically evaluated data, presented in a format that gives users ready access to the detailed vaporization chemistry and equilibrium partial pressures of the various species. To this end, we present graphs of species partial pressures as functions of temperature under representative reducing, neutral, and oxidizing environments. We also give equations for calculating partial pressures and maximum vaporization rates for arbitrary conditions of temperature and oxygen potential.

The present work is the second publication in a program sponsored by the Office of Standard Reference Data of the National Bureau of Standards to provide critically re-

viewed thermodynamic data of oxides, along with overviews of their high-temperature vaporization phenomena. The previous article (Lamoreaux and Hildenbrand, 1984) on alkali metal oxide systems discussed the scope of the program, the relevant literature, methods of data evaluation, and the mathematics of vaporization calculations. This article covers oxide systems of the elements Be, Mg, Ca, Sr, Ba, B, Al, Ga, In, Tl, Si, Ge, Sn, Pb, Zn, Cd, and Hg.

Readers should note that revised JANAF Thermodynamic Tables (Chase *et al.*, 1985), the final CODATA Key Values for Thermodynamics, and the CODATA Thermodynamic Tables (Garvin *et al.*, 1987) have been in preparation in the same time period as the present work and should appear concurrently. The minor differences in selected values of thermodynamic properties are immaterial to the purpose of this paper.

2. Properties of Individual Systems

2.1. Data Evaluation, Units, and Symbols

Molecular constants cited in the text are internuclear distances r in nm, vibrational wavenumbers ω in cm^{-1}, the molecular symmetry number σ, electronic state quantum weights g_i, and excited electronic state term values T_e in cm^{-1}. Thermodynamic quantities are expressed in dimensionless units, e.g., $S°/R$, $G°/RT$, or in kelvin units, e.g., $\Delta H°/R$, $\Delta G°/R$. The symbols K and kK, where 1 kK = 10^3 K, are used to represent kelvin units. Values of R used in the present work are 1.987 19 cal/mol K and 8.3144 J/mol K. The standard state pressure was taken as 1 atm ($1.013\,25 \times 10^5$ Pa), although the unit for computed vaporization partial pressures is the bar (10^5 Pa).

The thermodynamic symbols used in the present work are the following:

$\Delta_f H°_{298}/R$ — The standard molar enthalpy of formation at 298.15 K divided by the molar gas constant. Units = kelvins.

$(H°_{298} - H°_0)/R$ — The standard molar enthalpy increment between 0 and 298.15 K divided by the molar gas constant. Units = kelvins.

$-(G°_T - H°_{298})/RT$ — The standard molar Gibbs energy function divided by the molar gas constant.

$S°_T/R$ — The standard molar entropy at T K divided by the molar gas constant.

$T_{trs}, \Delta_{trs} H°/R$ — Solid-phase transition temperature and standard molar enthalpy of transition divided by the molar gas constant.

$T_{fus}, \Delta_{fus} H°/R$ — Melting temperature and standard molar enthalpy of fusion divided by the molar gas constant.

2.2. Thermodynamic Data and Vaporization Equilibria

Selected values of thermochemical properties of the relevant chemical species involved in the high-temperature vaporization equilibria are shown in Tables 1–3. Table 1 lists the reported melting points and enthalpies of fusion of high-temperature oxide phases. Table 2 presents Gibbs energy functions fit to the equation

$$-(G°_T - H°_{298})/RT = A + BT + CT^2 + DT^3 + ET^4 . \quad (1)$$

Values of $\Delta_f H°_{298}/R$, $S°_{298}/R$, and $(H°_{298} - H°_0)/R$ are presented in Table 3.

After careful review and comparison of the literature, Vols. 2 and 3 of the IVTAN compilation (Glushko *et al.*, 1978, 1979a, 1981, 1983) and recent JANAF (Stull *et al.*, 1971) supplements (Chase *et al.*, 1974, 1975, 1978, 1982, and dated individual issues) were chosen as the primary sources of data for the oxides of Be, Mg, Ca, Sr, Ba, B, Al, Ga, In, Tl, Si, Ge, Sn, and Pb. This choice was due to the uniform coverage of the recent literature and to the thoroughness of the reviews presented; agreement of recent JANAF issues with the IVTAN selected values is excellent. Other literature examined included reviews cited in the first paper (Brewer, 1953; Coughlin, 1954; Kelley, 1960; Schick, 1960; Ackermann and Thorn, 1961; Brewer and Rosenblatt, 1961; Kelley and King, 1961; Olette and Ancey-Moret, 1963; Wicks and Block, 1963; Brewer and Rosenblatt, 1969; Barin and Knacke, 1973; Samsonov *et al.*, 1978) and the 1982 NBS compilation (Wagman *et al.*, 1982). As described below, data from the selected sources were supplemented by our own analyses for a few of the minor gaseous species not

Table 1. Melting temperatures and enthalpies of fusion of oxide phases [a]

	T_{fus} (K)	$\Delta_{fus}H/R$ (kK)
BeO	2851 ± 12	10.3 ± 0.7
MgO	3100 ± 25	9.3 ± 0.7
CaO	2900 (-50,+300)	6.3 ± 0.6
SrO	2930 ± 30	8.4 ± 0.8
BaO	2290 ± 30	7.1 ± 0.7
B_2O_3	723 ± 1	2.95 ± 0.02
Al_2O_3	2327 ± 4	13.40 ± 0.36
Ga_2O_3	2080 ± 20	12.0 ± 2.4
In_2O_3	2186 ± 10	12.6 ± 1.2
Tl_2O	852 ± 10	3.64 ± 0.12
Tl_2O_3	1107 ± 10	6.37 ± 1.20
SiO_2(qu)	1726 ± 10	0.9 ± 0.1
SiO_2(cr)	1996 ± 5	1.15 ± 0.25
GeO_2	1388 ± 3	2.07 ± 0.3
SnO	1250 ± 30	3.33 ± 0.6
SnO_2	1903 ± 10	2.81 ± 0.6
PbO	1160 ± 10	3.08 ± 0.05
ZnO	2242 ± 25	
CdO	>1500	

[a] See Table 4 for references.

Table 2. Gibbs energy function equation parameters [a]

$(G°_T-H°_{298})/RT = A + BT + CT^2 + DT^3 + ET^4$

	A	10^3B	10^6C	10^9D	10^{12}E	T range,K
O(g)	20.151	-7.110	19.800	-18.16	5.987	298-1000
	18.210	3.296	-1.0262	0.2027	-0.01724	1000-3000
O_2(g)	25.757	-9.743	26.812	-24.157	7.8845	298-1000
	22.987	4.5769	-1.2107	0.2154	-0.01686	1000-3000
O_3(g)	30.370	-14.222	38.373	-33.85	10.885	298-1000
	26.052	7.018	-1.806	0.3086	-0.01934	1000-3000
Be(α)	2.034	-7.475	19.873	-17.976	5.957	298-1000
Be(α,β)	8.637	-24.584	31.968	-16.899	3.292	1000-1560
Be(l)	-3.236	7.078	-2.489	0.5080	-0.0430	1560-3000
Be(g)	17.144	-6.845	18.997	-17.344	5.697	298-1000
	15.252	3.199	-0.977	0.1904	-0.01602	1000-3000
BeO(s)	2.967	-10.99	28.75	-24.57	7.723	298-1000
	-0.674	5.719	-1.379	0.223	-0.0138	1000-2851
BeO(l)	-7.346	9.280	-1.810	0.21594	-0.01098	2851-4400
BeO(g)	24.867	-9.832	27.028	-24.330	7.933	298-1000
	21.073	4.6785	-1.4770	0.3178	-0.0291	1000-3000
Be_2O(g)	29.774	-20.1565	54.3939	-50.1244	16.7664	298-1000
	24.427	8.0534	-2.1884	0.3926	-0.0312	1000-3000
Be_2O_2(g)	32.854	-22.425	59.774	-54.066	17.870	298-1000
	26.667	9.150	-2.102	0.312	-0.020	1000-3000
Be_3O_3(g)	38.097	-33.9177	89.8539	-80.6047	26.4901	298-1000
	28.589	13.9546	-3.0033	0.4051	-0.0221	1000-3000
Be_4O_4(g)	40.566	-40.846	107.050	-94.434	30.696	298-1000
	28.776	17.0115	-3.0276	0.2743	-0.0017	1000-3000
Be_5O_5(g)	36.513	4.649	11.077	-5.7094	0.818	298-2900
Be_6O_6(g)	38.503	5.485	14.664	-7.0016	1.001	298-2900
Mg(s)	4.906	-8.577	23.50	-21.153	6.92	298-922
Mg(l)	0.000	8.49	-3.460	0.657		922-1500
Mg(g)	18.632	-6.845	18.997	-17.344	5.697	298-1000
	16.939	2.7458	-0.6073	0.06217		1000-3000
MgO(s)	4.853	-13.977	37.705	-33.422	10.77	298-1000
	0.762	6.6356	-1.7527	0.3108	-0.0238	1000-3100
MgO(l)	-0.804	5.1067	-0.3615			3100-3500
MgO(g)	26.832	-10.45	28.20	-24.40	7.81	298-1000
	23.16	5.90	-1.175	0.1043		1000-3000
Mg_2(g)	28.571	2.357	0.784	-0.597	0.0973	298-2900
Ca(s)	6.000	-8.551	22.703	-19.356	5.980	298-1115
Ca(l)	-0.150	11.003	-5.641	1.669	-0.205	1115-2000
Ca(g)	18.715	-2.045	7.181	-5.2376	1.29	298-1500
	17.84	2.537	-0.5155	0.0494		1500-3000
CaO(s)	6.367	-15.53	42.175	-37.723	12.225	298-1000
	1.882	7.3304	-2.0518	0.3837	-0.0316	1000-2900
CaO(l)	0.924	5.922	-0.7316	0.0436		2900-3800
CaO(g)	27.683	-11.194	30.70	-27.673	9.013	298-1000
	24.83	4.579	-0.9895	0.1144		1000-3000
Ca_2(g)	29.904	3.031	0.551	-0.5714	0.098	298-2900
Sr(s)	7.933	-10.5795	28.7422	-26.6189	8.9849	298-1041
Sr(l)	2.377	9.314	-4.345	1.2437	-0.1513	1041-2000
Sr(g)	20.556	-6.845	18.997	-17.344	5.697	298-1000
	18.670	3.179	-0.9560	0.1807	-0.01433	1000-3000
SrO(s)	8.476	-15.857	43.313	-38.867	12.64	298-1000
	3.963	7.379	-1.9765	0.367	-0.0304	1000-2930
SrO(l)	6.386	3.146				2930-3000
SrO(g)	28.947	-11.39	31.289	-28.261	9.22	298-1000
	25.602	5.676	-1.840	0.3974	-0.03455	1000-3000
Sr_2(g)	32.729	2.547	0.1393	-0.329	0.0609	298-2900
Sr_2O(g)	36.732	-22.190	60.226	-55.941	18.803	298-1000
	31.201	8.216	-2.092	0.328	-0.021	1000-3000
Ba(s)	8.902	-11.77	31.280	-27.375	8.74	298-1000
Ba(l)	3.426	9.095	-3.429	0.7557	-0.0695	1000-3000
Ba(g)	21.217	-6.78	18.914	-17.317	5.703	298-1000
	19.512	2.82	-0.6830	0.0871		1000-3000
BaO(s)	10.518	-16.350	44.77	-40.27	13.115	298-1000
	5.843	7.712	-2.160	0.4227	-0.0376	1000-2290
BaO(l)	1.172	9.907	-1.7986	0.1491		2290-3000
BaO(g)	29.592	-11.342	31.147	-28.132	9.177	298-1000
	26.393	5.305	-1.5133	0.2776	-0.02184	1000-3000
Ba_2(g)	36.295	-11.287	31.634	-30.544	10.529	298-1000
	33.641	4.200	-1.518	0.335	-0.031	1000-3000

Table 2. Gibbs energy function equation parameters (Continued)

$(G°_T-H°_{298})/RT = A + BT + CT^2 + DT^3 + ET^4$

	A	10^3B	10^6C	10^9D	10^{12}E	T range,K
Ba_2O(g)	37.386	-21.957	59.433	-55.081	18.489	298-1000
	31.635	8.710	-2.509	0.472	-0.039	1000-3000
Ba_2O_2(g)	41.823	-30.205	81.896	-76.084	25.574	298-1000
	33.968	11.925	-3.500	0.668	-0.056	1000-3000
B(s)	0.892	-1.883	4.894	-2.125		298-1000
	-0.229	2.270	-0.268	-.011	0.006	1000-2348
B(l)	-7.187	8.2687	-2.211	0.3219	-0.01906	2348-4300
B(g)	19.205	-6.828	18.957	-17.304	5.684	298-1000
	17.518	2.739	-0.6037	0.0616		1000-3000
BO(g)	25.538	-9.60	26.50	-23.978	7.85	298-1000
	22.855	4.4204	-1.1536	0.2032	-0.01593	1000-3000
BO_2(g)	29.430	-15.38	41.697	-36.995	11.94	298-1000
	24.906	7.330	-1.830	0.3033	-0.02227	1000-3000
B_2(g)	25.560	-11.10	30.027	-26.55	8.53	298-1000
	22.213	5.509	-1.503	0.274	-.022	1000-3000
B_2O(g)	29.513	-19.7041	53.1825	-48.9668	16.3750	298-1000
	24.277	7.8803	-2.1006	0.3700	-.0288	1000-3000
B_2O_2(g)	32.412	-21.030	57.385	-51.320	16.664	298-1000
	26.390	9.761	-2.4205	0.4048	-0.03025	1000-3000
B_2O_3(s)	11.447	-42.021	117.728	-123.930	49.645	298-723
B_2O_3(l)	-4.535	24.99	-9.642	2.399	-0.262	723-2000
B_2O_3(g)	37.087	-23.536	63.490	-55.990	18.015	298-1000
	30.144	11.050	-2.479	0.3720	-0.0248	1000-3000
Al(s)	4.343	-8.33	22.815	-20.497	6.705	298-933.61
Al(l)	-0.766	8.831	-3.7837	0.9296	-0.0931	933.61-2900
Al(g)	20.759	-8.4641	23.2158	-21.8534	7.4094	298-1000
	18.649	3.2317	-0.9905	0.193	-0.0162	1000-3000
AlO(g)	27.467	-10.673	29.229	-26.310	8.575	298-1000
	24.765	4.254	-0.8087	0.0793		1000-3000
AlO_2(g)	29.114	3.280	2.4785	-1.4446	0.22084	298-2900
Al_2(g)	29.637	-13.690	37.430	-33.720	10.970	298-1000
	25.767	6.399	-1.866	0.3566	-0.0299	1000-3000
Al_2O(g)	20.123	3.475	2.389	-1.4244	0.21605	298-2900
Al_2O_2(g)	32.197	4.484	3.337	-1.9575	0.2996	298-2900
Al_2O_3(s)	9.758	-31.19	83.503	-73.15	23.40	298-1000
	4.866	2.744	8.5295	-4.602	0.7695	1000-2327
Al_2O_3(l)	232.345	-336.622	193.672	-48.1032	4.4461	2327-3000
Ga(s)	6.263	-9.1060	15.305			298-302.92
Ga(l)	1.849	13.267	-12.531	7.426	-1.894	302.92-1000
	3.535	6.8206	-2.8728	0.7043	-0.0706	1000-3000
Ga(g)	21.361	-9.178	25.26	-23.064	7.552	298-1000
	18.828	4.302	-1.4845	0.3093	-0.02717	1000-2600
GaO(g)	29.008	-11.095	30.43	-27.423	8.95	298-1000
	25.976	4.886	-1.1755	0.1976	-0.0154	1000-3000
Ga_2O(g)	36.155	-17.11	46.857	-42.177	13.723	298-1000
	31.272	8.088	-2.305	0.4269	-0.0346	1000-3000
Ga_2O_3(s)	15.081	-41.0724	110.124	-100.900	33.6291	298-1000
	4.223	16.0456	-4.0362	0.6755	-0.0461	1000-2080
Ga_2O_3(l)	-10.389	29.837	-8.786	1.5334	-0.11264	2080-3000
In(s)	9.404	-19.929	50.346	-37.888		298-429.78
In(l)	4.824	6.051	-1.300	-0.896	0.500	429.78-1000
	4.868	6.448	-2.797	0.743	-0.083	1000-2400
In(g)	21.643	-6.722	18.523	-16.645	5.44	298-1000
	19.733	3.058	-0.6107	0.05655		1000-2400
InO(g)	30.031	-11.23	30.807	-27.77	9.074	298-1000
	26.955	4.92	-1.119	0.1685	-0.0115	1000-3000
In_2O(g)	37.892	-17.434	47.814	-43.124	14.05	298-1000
	32.940	8.220	-2.3696	0.4428	-0.0361	1000-3000
In_2O_3(s)	18.200	-44.122	118.710	-109.295	36.522	298-1000
	6.558	17.425	-4.7585	0.8572	-0.0665	1000-2186
In_2O_3(l)	-7.619	30.010	-8.791	1.522	-0.1108	2186-3000
Tl(s)	11.701	-36.5875	119.523	-164.816	86.659	298-576
Tl(l)	4.748	8.265	-4.264	1.295	-0.1576	576-1800
Tl(g)	22.520	-6.856	19.028	-17.381	5.712	298-1000
	20.659	3.087	-0.8375	0.1135		1000-1800
TlO(g)	31.052	-11.364	31.000	-27.614	8.946	298-1000
	27.683	5.489	-1.3467	0.2058	-0.0134	1000-3000
Tl_2O(s)	22.540	-42.731	119.855	-123.107	46.613	298-852
Tl_2O(l)	5.805	25.652	-10.338	2.4806	-0.2451	852-3000

Table 2.Gibbs energy function equation parameters (Continued)

	$(G°T-H°_{298})/RT = A + BT + CT^2 + DT^3 + ET^4$					
	A	10^3B	10^6C	10^9D	10^{12}E	T range,K
$Tl_2O(g)$	39.860	-17.750	48.76	-44.064	14.375	298-1000
	34.842	8.350	-2.4334	0.4584	-0.03765	1000-3000
$Tl_2O_3(s)$	23.752	-39.353	107.127	-96.004	31.16	298-1000
	13.305	15.999	-2.626			1000-1107
$Tl_2O_3(l)$	-0.743	40.917	-18.715	5.250	-0.627	1107-2000
Si(s)	3.101	-7.304	19.833	-17.696	5.73	298-1000
	1.052	3.254	-0.7263	0.0850		1000-1687
Si(l)	-8.152	13.849	-5.0426	0.961	-0.07316	1687-3600
Si(g)	20.984	-7.130	19.901	-18.28	6.03	298-1000
	19.039	3.32	-1.0484	0.2128	-0.0185	1000-3000
	19.959	1.9552	-0.2806	0.01899		3000-3600
SiO(g)	26.584	-10.123	27.756	-24.936	8.113	298-1000
	23.682	4.7876	-1.2880	0.2291	-0.01797	1000-3000
SiO_2(qu.)	6.947	-16.833	44.87	-38.893	12.413	298-1000
	1.394	9.002	-2.166	0.271		1000-1726
SiO_2(cr.)	7.605	-19.79	51.495	-44.403	13.91	298-1000
	1.937	8.590	-1.935	0.225		1000-1996
$SiO_2(l)$	2.120	7.6492	-1.2588	0.0998		1996-3000
$SiO_2(g)$	29.295	-15.684	42.55	-37.810	12.21	298-1000
	24.696	7.467	-1.898	0.3194	-0.0238	1000-3000
$Si_2(g)$	28.945	-11.627	31.790	-28.374	9.206	298-1000
	25.520	5.589	-1.3680	0.210	-0.01386	1000-3000
$Si_2O_2(g)$	40.398	-26.536	71.564	-65.861	22.009	298-1000
	33.340	10.626	-2.860	0.509	-0.040	1000-3000
$Si_3(g)$	34.400	-10.44	53.630	-49.516	15.863	298-1000
	29.042	9.140	-2.788	0.5832	-0.05276	1000-3000
Ge(s)	5.484	-15.1302	43.7517	-48.3508	20.0263	298-700
	2.896	1.8154	1.6677	-1.5224	0.3924	700-1210.4
Ge(l)	-5.426	15.1874	-6.5705	1.4859	-0.13343	1210.4-3200
Ge(g)	21.363	-10.534	29.285	-26.974	8.883	298-1000
	18.485	4.992	-1.8107	0.3906	-0.0351	1000-3200
GeO(g)	28.117	-10.587	29.000	-26.066	8.48	298-1000
	25.086	5.008	-1.385	0.251	-0.020	1000-3000
$GeO_2(s)$	7.621	-23.827	63.421	-57.714	19.138	298-1000
	118.948	-403.336	538.497	-313.567	68.097	1000-1388
$GeO_2(l)$	-7.387	21.608	-8.362	1.844	-0.167	1388-3000
$GeO_2(g)$	30.914	-16.700	45.425	-40.53	13.12	298-1000
	26.045	7.971	-2.142	0.3796	-0.0298	1000-3000
$Ge_2(g)$	32.229	-15.564	43.747	-40.584	13.465	298-1000
	28.103	7.132	-2.398	0.4977	-0.0437	1000-3000
$Ge_2O_2(g)$	40.990	-28.642	77.350	-71.242	23.759	298-1000
	33.146	12.193	-3.875	0.830	-0.079	1000-2000
Ge_3O_3	55.839	-48.258	130.774	-121.600	40.908	298-1000
	41.917	22.959	-9.814	3.022	-0.420	1000-2000
Sn(s)	9.860	-34.0554	110.534	-151.014	79.2152	298-505.12
Sn(l)	1.684	14.256	-11.690	5.627	-1.122	505.12-1400
	4.201	6.483	-2.3645	0.5071	-0.0450	1400-3000
Sn(g)	21.052	-6.998	18.881	-16.378	5.221	298-1000
	18.77	3.667	-0.7262	0.0646		1000-3000
SnO(s)	10.425	-30.8313	89.3685	-99.1119	41.2146	298-700
	4.990	4.5034	1.9568	-2.0117	0.5137	700-1250
SnO(l)	-3.168	19.3711	-9.1257	2.5224	-0.2917	1250-2000
SnO(g)	29.148	-10.96	30.054	-27.070	8.816	298-1000
	26.025	5.173	-1.461	0.2692	-0.0217	1000-3000
$SnO_2(s)$	8.410	-21.510	57.480	-50.560	16.203	298-1000
	2.201	9.676	-2.092	0.236		1000-1903
$SnO_2(l)$	-1.715	13.943	-3.931	0.6916	-0.0523	1903-3000

Table 2.Gibbs energy function equation parameters (Continued)

	$(G°T-H°_{298})/RT = A + BT + CT^2 + DT^3 + ET^4$					
	A	10^3B	10^6C	10^9D	10^{12}E	T range,K
$SnO_2(g)$	32.251	-17.54	47.834	-42.85	13.90	298-1000
	27.190	8.322	-2.301	0.4159	-0.033	1000-3000
$Sn_2(g)$	32.827	-12.85	34.68	-30.297	9.65	298-1000
	28.634	7.03	-1.967	0.3357	-0.0245	1000-3000
$Sn_2O_2(g)$	35.752	6.440	1.070	-1.011	0.171	298-3000
$Sn_3O_3(g)$	44.474	0.177	14.80	-7.926	1.264	298-3000
$Sn_4O_4(g)$	51.729	6.476	9.775	-5.144	0.772	298-3000
Pb(s)	9.762	-17.085	49.44	-54.63	22.66	298-600.65
Pb(l)	4.814	8.045	-3.983	1.191	-0.1493	600.65-2200
Pb(g)	21.847	-6.85	19.007	-17.354	5.70	298-1000
	19.914	3.308	-1.080	0.2288	-0.0197	1000-3000
PbO(red)	11.492	-28.7693	82.3965	-89.2160	36.1111	298-762
PbO(yel)	6.081	4.9700	1.5284	-1.8198	0.4842	762-1160
PbO(l)	-1.494	19.2561	-9.2613	2.6476	-0.3178	1160-2000
PbO(g)	30.128	-11.204	30.750	-27.740	9.040	298-1000
	26.949	5.276	-1.5062	0.2792	-0.0225	1000-3000
$PbO_2(s)$	10.231	-15.016	41.48	-33.24	9.446	298-1200
$PbO_2(g)$	33.462	-18.196	49.746	-44.714	14.536	298-1000
	28.252	8.606	-2.440	0.450	-0.0364	1000-3000
$Pb_2(g)$	34.777	-12.426	34.43	-31.38	10.30	298-1000
	31.381	5.687	-1.6535	0.3116	-0.02454	1000-3000
$Pb_2O_2(g)$	35.958	4.176	7.238	-4.146	0.658	298-3000
$Pb_2O_3(s)$	24.026	-48.4163	129.197	-117.502	39.0413	298-1000
$Pb_3O_3(g)$	44.777	6.271	10.844	-6.210	0.985	298-3000
$Pb_3O_4(s)$	26.958	-20.333	64.277	-45.386	11.00	298-1500
$Pb_4O_4(g)$	50.677	8.367	14.449	-8.274	1.312	298-3000
$Pb_5O_5(g)$	54.313	10.462	18.055	-10.338	1.639	298-3000
$Pb_6O_6(g)$	62.478	12.557	21.661	-12.401	1.966	298-3000
Zn(s)	5.763	-6.350	15.47	-8.73		298-692.73
Zn(l)	1.150	9.66	-4.862	1.132		692.73-1200
Zn(g)	19.791	-4.396	12.606	-10.378	3.000	298-1200
	18.184	3.2905	-1.0522	0.2166	-0.01932	1200-3000
ZnO(s)	8.676	-29.783	86.988	-98.618	42.157	298-693
	3.215	5.346	-0.145	-0.494	0.123	693-2000
ZnO(g)	28.337	-11.610	31.807	-28.827	9.43	298-1000
	25.163	5.166	-1.4237	0.2511	-0.01924	1000-3000
Cd(s)	5.195	10.13	-40.49	74.52	-45.76	298-594.26
Cd(l)	2.511	10.22	-5.823	1.538		594.26-1100
Cd(g)	20.748	-5.4625	15.305	-13.216	4.055	298-1100
	19.318	2.349	-0.035	-0.263	0.064	1100-2000
CdO(s)	6.887	-5.035	16.921	-12.132	2.97	298-1500
CdO(g)	29.305	-11.443	31.53	-28.494	9.29	298-1000
	26.054	5.467	-1.6246	0.3137	-0.0266	1000-3000
Hg(l)	10.797	-14.507	41.32	-43.32	16.75	298-800
Hg(g)	21.798	-6.845	18.997	-17.344	5.697	298-1000
	19.906	3.195	-0.9736	0.1891	-0.01585	1000-3000
HgO(s)	10.251	-15.674	42.5	-37.73	12.18	298-1000
HgO(g)	27.982	2.237	1.41	-0.8606	0.1332	298-2900

[a]See Table 4 for references.

Table 3. Values of $\Delta_f H°_{298}/R$, $S°_{298}/R$, and $(H°_{298}-H°_0)/R$ [a]

	$\Delta_f H°_{298}/R$ (kK)	$S°_{298}/R$	$(H°_{298}-H°_0)/R$ (kK)
O(g)	29.97 ± 0.01	19.3578 ± 0.0001	0.8092
O_2(g)		24.660 ± 0.004	1.0440
O_3(g)	17.1 ± 0.2	28.73 ± 0.01	1.2468
Be(α)		1.143 ± 0.006	0.2345
Be(g)	39.0 ± 0.6	16.3770 ± 0.0001	0.74538
BeO(s)	-73.29 ± 0.3	1.656 ± 0.005	0.3412
BeO(g)	16.1 ± 1.	23.756 ± 0.05	1.0449
Be_2O(g)	-4.5 ± 0.3	27.403 ± 0.3	1.3459
Be_2O_2(g)	-46.3 ± 3.	30.19 ± 0.3	1.4697
Be_3O_3(g)	-123. ± 4.	34.045 ± 0.3	1.819
Be_4O_4(g)	-198. ± 5.	35.644 ± 0.3	1.9044
Be_5O_5(g)	-265. ± 15.	(36.67) ± 0.3	2.290
Be_6O_6(g)	-330. ± 15.	(41.26) ± 0.5	2.583
Mg(s)		3.931 ± 0.01	0.6014
Mg(g)	17.7 ± 0.1	17.8651 ± 0.0001	0.74538
MgO(s)	-72.34 ± 0.04	3.24 ± 0.02	0.6206
MgO(g)	7.0 ± 3.	25.637 ± 0.01	1.0715
Mg_2(g)	34.7 ± 0.3	29.33 ± 0.05	1.2409
Ca(s)		5.003 ± 0.04	0.689
Ca(g)	21.4 ± 0.1	18.6154 ± 0.0004	0.74538
CaO(s)	-76.384 ± 0.1	4.582 ± 0.02	0.812
CaO(g)	5.3 ± 2.	26.412 ± 0.05	1.077
CaO_2(s)	-79.6 ± 0.3	(7.8) ± 0.3	
Ca_2(g)	41.6 ± 0.4	30.842 ± 0.2	1.316
Sr(s)		6.70 ± 0.02	0.7902
Sr(g)	19.8 ± 0.5	19.7886 ± 0.0002	0.74538
SrO(s)	-71.0 ± 0.1	6.668 ± 0.06	1.042
SrO(g)	-0.2 ± 3.	27.656 ± 0.002	1.0873
SrO_2(s)	-77. ± 2.	(11.) ± 0.5	
Sr_2(g)	37.3 ± 0.6	33.493 ± 0.6	1.3237
Sr_2O(g)	-25.4 ± 3.	34.1 ± 1.	1.535
Ba(s)		7.517 ± 0.08	0.8311
Ba(g)	21.9 ± 1.	20.4627 ± 0.0001	0.74538
BaO(s)	-65.9 ± 0.3	8.66 ± 0.05	1.198
BaO(g)	-15.4 ± 1.	28.306 ± 0.05	1.084
Ba_2(g)	41.9 ± 0.8	35.015 ± 0.6	1.3172
Ba_2O(g)	-29. ± 5.	34.8 ± 1.	1.429
Ba_2O_2(g)	-72. ± 5.	38.3 ± 1.	1.882
B(s)		0.710 ± 0.01	0.1470
B(g)	67.9 ± 0.5	18.441 ± 0.001	0.7603
BO(g)	1.2 ± 1.	24.458 ± 0.003	1.0433
BO_2(g)	-39.0 ± 2.	27.665 ± 0.01	1.2956
B_2(g)	99.8 ± 4.	24.291 ± 0.1	1.0598
B_2O(g)	33. ± 12.	27.20 ± 0.50	1.4172
B_2O_2(g)	-55.5 ± 1.	30.015 ± 0.2	1.6112
B_2O_3(s)	-153.17 ± 0.17	6.491 ± 0.04	1.1187
B_2O_3(g)	-100.5 ± 0.5	34.371 ± 0.5	1.7341
Al(s)		3.405 ± 0.01	0.5490
Al(g)	39.60 ± 0.3	19.7782 ± 0.0001	0.8322
AlO(g)	8.1 ± 1.	26.25 ± 0.01	1.0568
AlO_2(g)	-10.4 ± 4.	(30.27) ± 1.	1.4483
Al_2(g)	59.0 ± 2.5	28.075 ± 0.03	1.1808
Al_2O(g	-17.5 ± 2.	30.33 ± 0.4	1.5288
Al_2O_2(g)	-47.5 ± 4.	(33.78) ± 1.5	1.7462
Al_2O_3(s)	-201.54 ± 0.15	6.127 ± 0.01	1.2047
Ga(s)		4.993 ± 0.04	0.675

Table 3. Values of $\Delta_f H°_{298}/R$, $S°_{298}/R$, and $(H°_{298}-H°_0)/R$ (Continued)

	$\Delta_f H°_{298}/R$ (kK)	$S°_{298}/R$	$(H°_{298}-H°_0)/R$ (kK)
Ga(g)	32.7 ± 0.5	20.3180 ± 0.0002	0.7879
GaO(g)	17.7 ± 3.	27.749 ± 0.006	1.0734
Ga_2O(g)	-11.46 ± 1.	34.21 ± 0.4	1.4712
Ga_2O_3(s)	-131.2 ± 0.5	10.216 ± 0.04	1.750
In(s)		6.934 ± 0.03	0.7950
In(g)	28.9 ± 0.1	20.8878 ± 0.0001	0.7455
InO(g)	20.5 ± 3.	28.76 ± 0.06	1.081
In_2O(g)	-5.17 ± 2.	35.91 ± 0.4	1.5087
In_2O_3(s)	-111.4 ± 0.2	13.00 ± 0.4	2.0807
Tl(s)		7.734 ± 0.02	0.8217
Tl(g)	21.7 ± 0.2	21.7522 ± 0.0001	0.74538
TlO(g)	23.6 ± 5.	29.76 ± 1.	1.0904
Tl_2O(s,l)	-20.1 ± 0.2	17.56 ± 1.	1.816
Tl_2O(g)	3.7 ± 1.	37.85 ± 0.6	1.554
Tl_2O_3(s)	-46.5 ± 0.5	19.244 ± 1.	2.4295
Si(s)		2.262 ± 0.01	0.3869
Si(g)	54.2 ± 1.	20.1903 ± 0.0001	0.9081
SiO(g)	-11.9 ± 0.6	25.437 ± 0.002	1.0482
SiO_2(qu)	-109.53 ± 0.1	4.99 ± 0.02	0.8318
SiO_2(g)	-38.7 ± 1.	27.496 ± 0.1	1.268
Si_2(g)	67.9 ± 2.	27.625 ± 0.1	1.1141
Si_2O_2(g)	-43.22 ± 2.	37.3 ± 3.	1.835
Si_3(g)	74. ± 3.	32.3 ± 0.60	1.6783
Ge(s)		3.74 ± 0.02	0.5576
Ge(g)	44.7 ± 0.4	20.181 ± 0.001	0.8808
GeO(g)	-4.5 ± 0.5	26.915 ± 0.005	1.0562
GeO_2(tet)	-69.78 ± 0.1	4.776 ± 0.02	0.8696
GeO_2(g)	-13. ± 2.	29.00 ± 0.1	1.354
Ge_2(g)	58. ± 1.	30.508 ± 0.001	1.3983
Ge_2O_2(g)	-33. ± 2.	37.6 ± 1.5	1.900
Ge_3O_3(g)	-59.6 ± 2.	50.2 ± 2.5	3.250
Sn(s)		6.156 ± 0.01	0.7605
Sn(g)	36.23 ± 0.1	20.2517 ± 0.0004	0.7475
SnO(s)	-33.76 ± 0.02	6.876 ± 0.035	1.0507
SnO(g)	2.6 ± 0.5	27.904 ± 0.005	1.0663
SnO_2(s)	-69.47 ± 0.02	5.895 ± 0.01	1.0084
SnO_2(g)	-5. ± 6.	30.248 ± 0.5	1.4186
Sn_2(g)	49.6 ± 1.	31.352 ± 0.1	1.235
Sn_2O_2(g)	-29. ± 2.	37.7 ± 3.	
Sn_3O_3(g)	-61. ± 3.	45.6 ± 4.	
Sn_4O_4(g)	-95. ± 3.	54.4 ± 4.	
Pb(s)		7.794 ± 0.035	0.8263
Pb(g)	23.48 ± 0.1	21.080 ± 0.001	0.74538
PbO(red)	-26.29 ± 0.06	8.16 ± 0.02	1.1095
PbO(g)	8.2 ± 1.	28.857 ± 0.003	1.0778
PbO_2(g)	0.8 ± 6.	31.39 ± 0.1	1.4735
PbO_2(s)	-33.1 ± 0.3	8.635 ± 0.02	1.3184
Pb_2(g)	35.9 ± 0.3	33.383 ± 0.1	1.270
Pb_2O_2(g)	-15. ± 3.	37.3 ± 3.	
Pb_2O_3(s)	-59.1 ± 0.4	18.27 ± 0.25	2.5113
Pb_3O_3(g)	-38. ± 4.	47.5 ± 4.	
Pb_3O_4(s)	-86.4 ± 0.8	25.49 ± 0.3	3.6308
Pb_4O_4(g)	-68. ± 6.	54.2 ± 5.	
Pb_5O_5(g)	-93. ± 6.	58.8 ± 6.	
Pb_6O_6(g)	-119. ± 6.	67.8 ± 6.	

Table 3. Values of $\Delta_f H°_{298}/R$, $S°_{298}/R$, and $(H°_{298}-H°_0)/R$. (Continued)

	$\Delta_f H°_{298}/R$ (kK)	$S°_{298}/R$	$(H°_{298}-H°_0)/R$ (kK)
Zn(s)		5.017 ± 0.02	0.6804
Zn(g)	15.69 ± 0.02	19.3494 ± 0.0002	0.74538
ZnO(s)	-42.15 ± 0.03	5.25 ± 0.05	0.8339
ZnO(g)	10.9 ± 1.	26.95 ± 0.3	1.082
Cd(s)		6.230 ± 0.02	0.7513
Cd(g)	13.45 ± 0.08	20.1623 ± 0.0001	0.74538
CdO(s)	-31.04 ± 0.1	6.59 ± 0.20	1.011
CdO(g)	15.6 ± 1.	(28.014) ± 0.1	1.104
Hg(l)		9.13 ± 0.01	1.1236
Hg(g)	7.382 ± 0.005	21.0310 ± 0.0002	0.74542
HgO(s)	-10.92 ± 0.01	8.45 ± 0.04	1.0965
HgO(g)	11.2 ± 1.0	28.86 ± 0.3	1.082

[a]See Table 4 for references.

included in the major compilations. In all cases, the thermodynamic values selected reproduce, within experimental uncertainty, the vapor pressure measurements considered reliable.

In reviewing the available tabulations of thermodynamic functions for gaseous atoms, it was discovered that heat capacity, Gibbs energy function, entropy, and enthalpy increment values for many elements are in error because they are based on only the observed electronic levels, e.g., as listed by Moore (1949, 1952, 1958), and do not include unobserved low-lying levels, which can contribute significantly. Although this problem was not severe for the elements covered in this paper, it should be noted that the equations for Gibbs energy functions given for gaseous atoms in Table 2 are consistent with new calculations that take into account more recent spectroscopic data and estimates of missing low-lying electronic levels (Brewer, 1983). The equations given for $-(G°_T - H°_{298})/RT$ represent the tabulated values within typical limits of ± 0.01 over their applicable temperature ranges. The equations were derived by fitting tabular data and are not direct integrations of heat capacity equations. Because of the nature of the polynomial fits, values derived by differentiating these equations do not represent thermodynamic properties, e.g., heat capacities, accurately.

Data sources for each of the selected values are in any case summarized in Table 4, and more complete discussions of data sources are given below, when necessary.

The calculated partial pressures of major gaseous species in equilibrium with stable condensed oxide phases are shown below as plots of log P vs $1/T$ for several representative vaporization conditions. The particular conditions are 0.2 bar O_2, representing oxidizing conditions, congruent vaporization, representing neutral vaporization, and either 10^{-15} bar O_2 or the O_2 pressure of the metal–metal oxide equilibria, representing reducing conditions. The metal–metal oxide equilibrium O_2 pressure was chosen when it exceeded 10^{-15} bar. The maximum vaporization rates calculated by the Hertz–Knudsen equation are also shown in plots below.

TABLE 4. Sources of data in Tables 1 through 3[a]

	$-(G°T-H°_{298})/T$ $S°_{298}, H°_{298}-H°_0$	$\Delta_f H°_{298}$	T_{fus}
O(g)	6,25	7	
O_2(g)	6,25		
O_3(g)	25	25	
Be(α)	1(2),7,8,9,14		
Be(g)	1,2,7,8,10,14	7,8,1,9,14	
BeO(s)	1,5,7(9),14	7,1,5,9,14	1
BeO(g)	1,5,14	1,5,14	
Be_2O(g)	1	1	
Be_2O_2(g)	1	1	
Be_3O_3(g)	1	1	
Be_4O_4(g)	1	1	
Be_5O_5(g)	2	b	
Be_6O_6(g)	2,14	b	
Mg(s)	2(1),7,8,14		2
Mg(g)	1,8,2,7,9,10,14	7,1,2(8),9,14	
MgO(s)	1,5,7,9,14	7,1,5,9,14	1,19
MgO(g)	5,1,14	5,1,14	
Mg_2(g)	5(1)	5(1)	
Ca(s)	1,7,2,8,9,14		1
Ca(g)	1,2,7,8,9,10,14	7,11,1,8,9,14	
CaO(s)	1(4),7,14	7,1,4,9,14	1
CaO(g)	5,1,14	5,1,14	
CaO_2(s)		26(9)	
Ca_2(g)	5(1),14	5(1),14	
Sr(s)	1(2),(9,14)		1
Sr(g)	1,3(8),9,10,14	11(1,9,14)	
SrO(s)	1,4(9,14)	1,4,9,14	1
SrO(g)	1,4,14	27,4(9),14	
SrO_2(s)		12(9)	
Sr_2(g)	1	1	
Sr_2O(g)	b	b	
Ba(s)	1,4,9,14		1
Ba(g)	10,1,4,9,10,14	8,11(1,3,9,14)	
BaO(s)	1,4(9,14)	1,4(9),14	1
BaO(g)	1,4,14	1(4),14	
Ba_2(g)	1	1	
Ba_2O(g)	b	b	
Ba_2O_2(g)	b	b	
B(s)	13,1,7,8,9,14		13
B(g)	13,1,7,8,9,10,14	11,1,7,9(13)	
BO(g)	1,2,9,14	1,2,14	
BO_2(g)	1,2,9,14	1	
B_2(g)	1,13	13,1	
B_2O(g)	1,2,14	1	
B_2O_2(g)	1(2),(9)	1,2(9)	
B_2O_3(s)	1,3,7,9,14	1,3,7,9,14	1
B_2O_3(g)	1,3(9)	1,3,7,9	
Al(s)	28,1,7,8,9,14,17		28
Al(g)	17,1,7,8,10,14	28,1,7,8,14,17	
AlO(g)	17(1)	17,1	
AlO_2(g)	17(1)	17(1)	
Al_2(g)	1	1	
Al_2O(g)	17(1)	17(1)	
Al_2O_2(g)	17,1	17,1	
Al_2O_3(s)	17,1,7,9,14	7,17,1,9,14	1,19
Ga(s)	1,22,8,9,14		1
Ga(g)	1,8(9),10,14	1,8(9),14	
GaO(g)	1,9	1	
Ga_2O(g)	1	1	
Ga_2O_3(s)	1,9,14	1,9,14	1
In(s)	1,8(9),14		1
In(g)	8,1,9,10,14	1,8,9,14	
InO(g)	1	1	
In_2O(g)	1	1	
In_2O_3(s)	1	1,9	1
Tl(s)	8,1,9,14		1
Tl(g)	8,1,9,10,14	8,11,1,9,14	
TlO(g)	1	1	
Tl_2O(s)	1	1(14)	1

TABLE 4. (*continued*)

	$-(G°T-H°_{298})/T$ $S°_{298},H°_{298}-H°_0$	$\Delta_f H°_{298}$	T_{fus}
$Tl_2O(g)$	1(14)	1	
$Tl_2O_3(s)$	1(14)	1(14)	1
Si(s)	21,26,8,14,16		21
Si(g)	16,2,7,8,9,10,14	2,7,16	
SiO(g)	16,2,9,14	16(2),9,14	
SiO_2(qu)	[b]	7,2,9,14,16	19,2
SiO_2(cr)	[b]	[b]	16,2
$SiO_2(g)$	16,2,14	16,2,9,14,	
$Si_2(g)$	16,2,9,14	16	
$Si_2O_2(g)$	[b]	[b]	
$Si_3(g)$	23,2,14,16	8,2,14,16	
Ge(s)	8,16,7,9,14		16
Ge(g)	16,8,9,10,14	16(8,9,14)	
GeO(g)	12,16(9)	12,16(9)	
$GeO_2(s)$	16,7,14	7,14,16	16
$GeO_2(g)$	16	16	
$Ge_2(g)$	16,9	16	
$Ge_2O_2(g)$	[b]	[b]	
$Ge_3O_3(g)$	[b]	[b]	
Sn(s)	8,16,7,9,14		16
Sn(g)	8,16,9,10,14	7,16,8(9),14,16	
SnO(s)	16,7(9),14	16(7,9,14)	16
SnO(g)	16,9	16(9)	
$SnO_2(s)$	16(7,9,14)	16(7,9,14)	16
$SnO_2(g)$	16	16	
$Sn_2(g)$	16,18	18,16	
$Sn_2O_2(g)$	[b]	[b]	
$Sn_3O_3(g)$	[b]	[b]	
$Sn_4O_4(g)$	[b]	[b]	
Pb(s)	16,7,8,9,14		16
Pb(g)	16,10(2,8,9,14)	7,8,9,14,16	
PbO(red)	16,3,9,14	3,16,9,14	
PbO(yel)	16,3,14	16,2,20	16
PbO(g)	16,3,14	3,16,14	
$PbO_2(s)$	3,14,16	3,16,14	
$PbO_2(g)$	16	16	
$Pb_2(g)$	16,18	18,16	
$Pb_2O_2(g)$	[b]	[b]	
$Pb_2O_3(s)$	16,9	16	
$Pb_3O_3(g)$	[b]	[b]	
$Pb_3O_4(s)$	3,9,14,16	3,16,9,14	
$Pb_4O_4(g)$	[b]	[b]	
$Pb_5O_5(g)$	[b]	[b]	
$Pb_6O_6(g)$	[b]	[b]	
Zn(s)	15(8),(14)		15
Zn(g)	15,8,10,14	7,8,9,14,15	
ZnO(s)	7,14	7(9),14	20

TABLE 4. (*continued*)

	$-(G°T-H°_{298})/T$ $S°_{298},H°_{298}-H°_0$	$\Delta_f H°_{298}$	T_{fus}
ZnO(g)	[b]	[b]	
Cd(s)	8,14		8
Cd(g)	8,7,10,14	8,7,14	
CdO(s)	14,7	7,14	20
CdO(g)	[b]	[b]	
Hg(l)	8,2,14		
Hg(g)	2,8,7,10,14	7,2,8,14	
HgO(s)	2,7,14	7,2,14	
HgO(g)	[b]	[b]	

References to Table 4

[1](Glushko *et al.*, 1981).
[2](Stull *et al.*, 1971).
[3](Chase *et al.*, 1974).
[4](Chase *et al.*, 1975).
[5](Chase *et al.*, 1978).
[6](Chase *et al.*, 1982).
[7](Cox, 1978).
[8](Hultgren and Desai, 1973).
[9](Wagman *et al.*, 1982).
[10](Brewer, 1983).
[11](Brewer, 1977).
[12](Brewer and Rosenblatt, 1969).
[13](Stull *et al.*, 1971, 31 March 1979 unbound supplement).
[14](Pankratz, 1982).
[15](Stull *et al.*, 1971, 31 December 1978 unbound supplement).
[16](Glushko *et al.*, 1979a).
[17](Stull *et al.*, 1971, 31 December 1979 unbound supplement). JANAF issued two sets of supplements on Al–O species dated 1979; the later set, with references to literature as late as 1982, is cited.
[18](Balasubramanian and Pitzer, 1983).
[19](Hlavac, 1982).
[20](Shunk, 1969).
[21](Desai, 1986a).
[22](Amitin *et al.*, 1984).
[23](Brewer, 1984).
[24](Richet *et al.*, 1982).
[25](Glushko *et al.*, 1978).
[26](Glushko *et al.*, 1979b).
[27](Murad, 1981).
[28](Desai, 1986b).

[a] References without parentheses are in essential agreement; those in parentheses differ from the chosen value by a significant portion of the stated uncertainty. The sources of the selected data are in boldface.
[b] See text.

a. Be–O System

The only high-temperature solid phase is the oxide, BeO. Under neutral and reducing conditions, vaporization takes place primarily by decomposition to Be atoms and oxygen species. BeO, Be_2O_2, Be_3O_3, Be_4O_4, and Be_5O_5 are the principal vapor species under oxidizing conditions. Partial pressures of major vapor species and calculated maximum vaporization rates are shown in Figs. 1–4.

$Be_5O_5(g)$, $Be_6O_6(g)$ thermodynamic data—the enthalpy of formation was calculated by the third-law method using the mass spectrometric data of Chupka, Berkowitz, and Giese (1959) and of Theard and Hildenbrand (1964).

b. Mg–O System

The only high-temperature solid phase is the oxide, MgO. In neutral and reducing atmospheres, vaporization takes place by dissociation to give gaseous oxygen species and Mg(g); the MgO(g) partial pressure is comparable to that of Mg(g) in oxidizing atmospheres. Partial pressures of major vapor species and calculated maximum vaporization rates are shown in Figs. 5–8. As can be seen from the graphs, MgO is especially volatile at high temperatures under reducing conditions. This has important practical consequences in pointing out the instability and limited usefulness of magnesia-based refractories in hydrogen-containing or otherwise

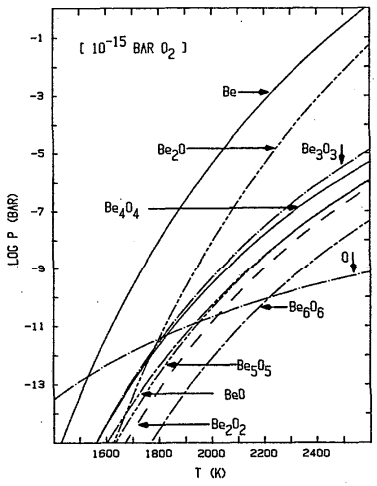

FIG. 1. BeO vaporization in 10^{-15} bar O_2.

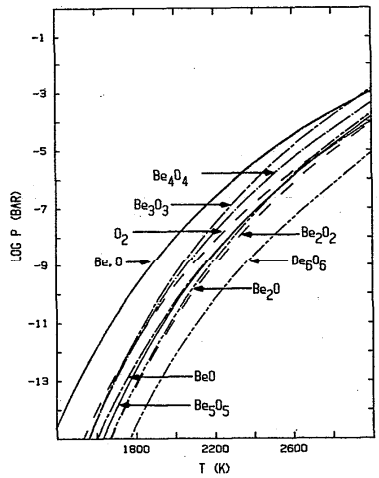

FIG. 2. BeO congruent vaporization.

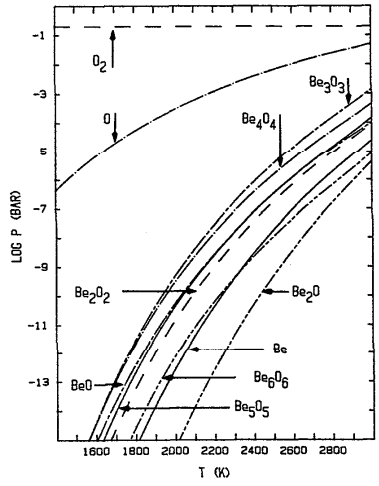

FIG. 3. BeO vaporization in 0.2 bar O_2.

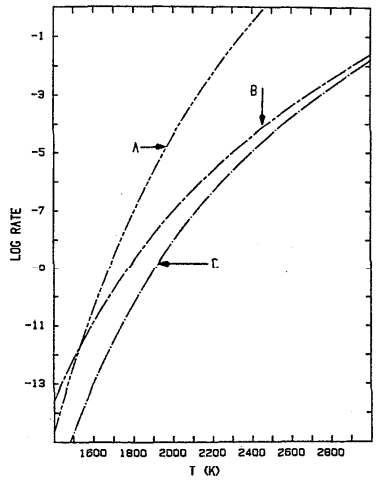

FIG. 4. BeO maximum vaporization rates. A—10^{-15} bar O_2; B—congruent vaporization; C—0.2 bar O_2.

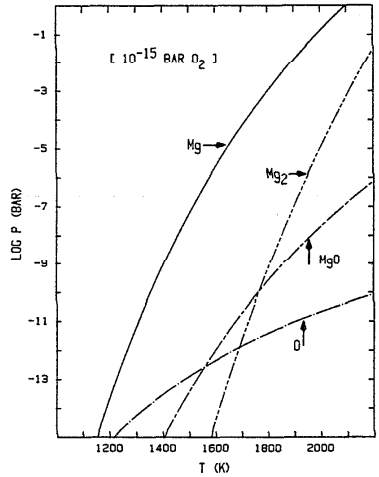

FIG. 5. MgO vaporization in 10^{-15} bar O_2.

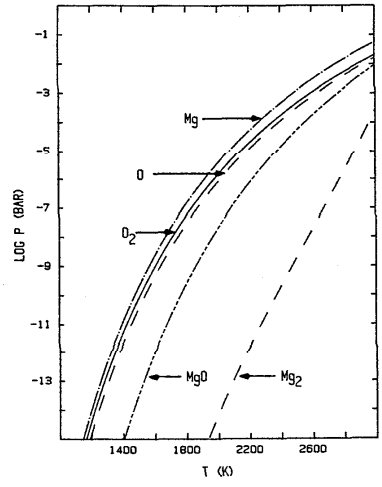

FIG. 6. MgO congruent vaporization.

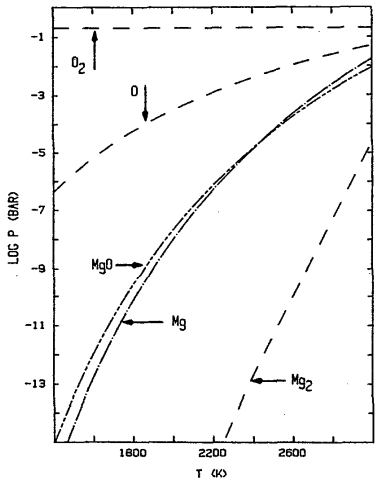

FIG. 7. MgO vaporization in 0.2 bar O_2.

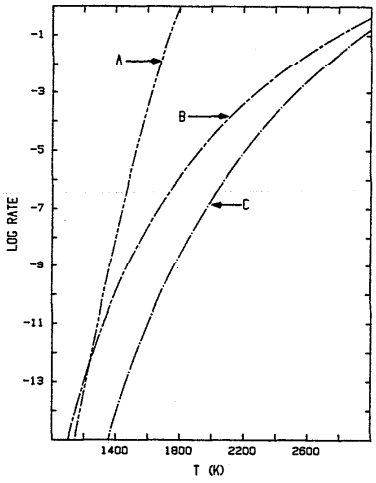

FIG. 8. MgO maximum vaporization rates. A—10^{-15} bar O_2; B—congruent vaporization; C—0.2 bar O_2.

reducing atmospheres. The same is true of several of the other alkaline earth oxides.

c. Ca–O System

The only high-temperature solid phase is the oxide, CaO. The equilibrium oxygen pressure of the peroxide, CaO_2, exceeds 0.2 bar at temperatures above about 300 K (Vannerberg, 1962). Vaporization takes place primarily by dissociation to Ca(g) and oxygen under neutral and reducing conditions; CaO(g) is the primary vapor phase product in oxidizing atmospheres. Partial pressures of major vapor species and calculated maximum vaporization rates are shown in Figs. 9–12.

d. Sr–O System

SrO(s) is the stable high-temperature condensed phase under neutral and reducing conditions. SrO_2(s) is stable in oxidizing atmospheres at lower temperatures; the O_2 pressure over SrO_2(s) reaches 0.2 bar at about 800 K (Vannerberg, 1962). Vaporization takes place primarily by dissociation to Sr(g), SrO(g), and oxygen species under neutral and oxidizing conditions, while sublimation to SrO(g) dominates in oxidizing atmospheres. The calculated neutral vapor composition is consistent with the observation of Kaufman *et al.* (1965) from electric deflection experiments that the vapor at 2500 K contains about 5 mol % molecular SrO. Partial pressures of major vapor species and calculated maximum vaporization rates are shown in Figs. 13–16.

Sr_2O(g) thermodynamic data—although Sr_2O is not a major species and is not listed in the IVTAN or JANAF compilations, the results of Drowart *et al.* (1964) indicate that it should be included for completeness. Therefore, their estimated molecular constants were adopted and used to evaluate thermodynamic functions: $\angle$Sr–O–Sr = 180°, r(Sr–O) = 0.192 nm, vibrational fundamentals of 256, 233 (doubly degenerate), and 888 cm^{-1}, an electronic ground state degeneracy of 3, and no excited electronic states. The enthalpy of formation of Sr_2O(g) was derived from a third-

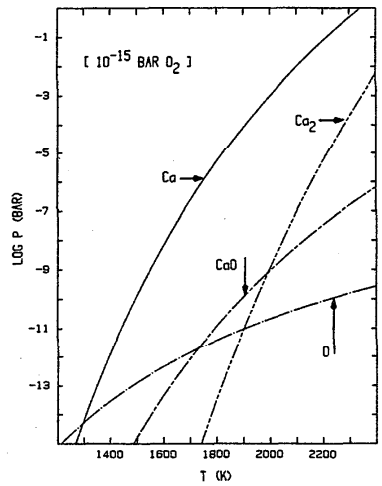

FIG. 9. CaO vaporization in 10^{-15} bar O_2.

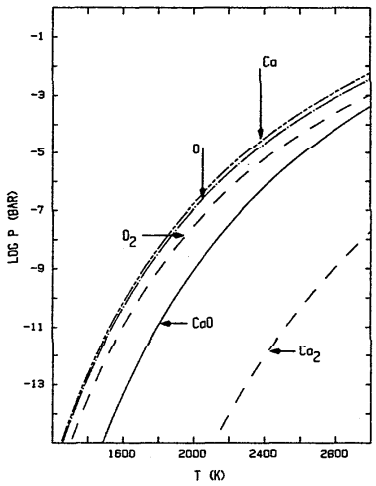

FIG. 10. CaO congruent vaporization.

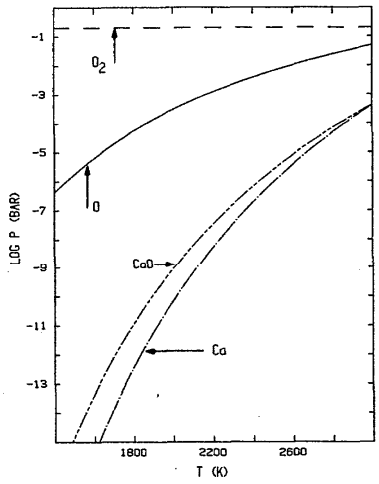

FIG. 11. CaO vaporization in 0.2 bar O_2.

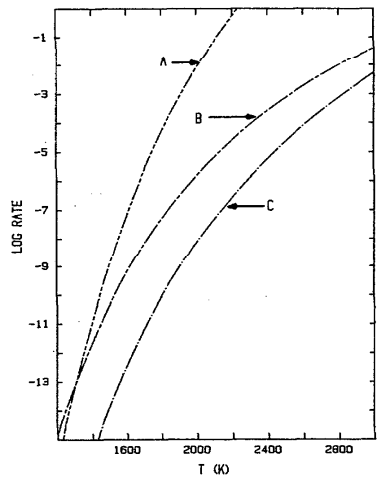

FIG. 12. CaO maximum vaporization rates. A—10^{-15} bar O_2; B—congruent vaporization; C—0.2 bar O_2.

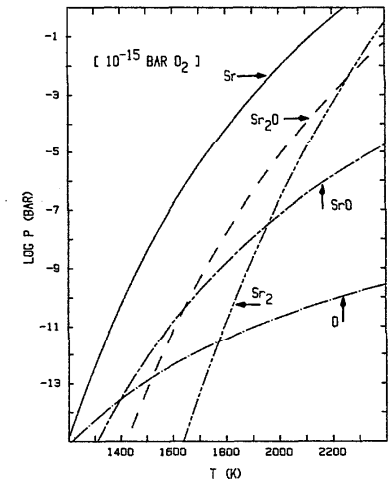

FIG. 13. SrO vaporization in 10^{-15} bar O_2.

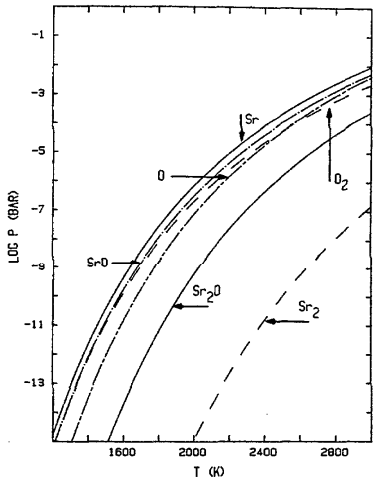

FIG. 14. SrO congruent vaporization.

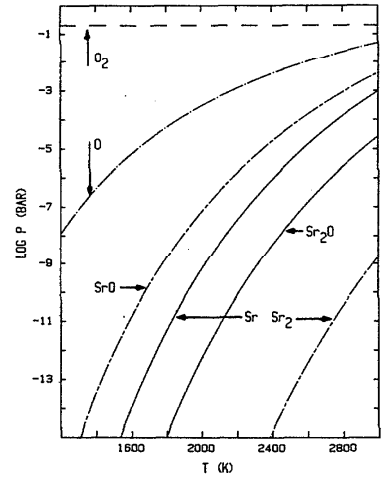

FIG. 15. SrO vaporization in 0.2 bar O_2.

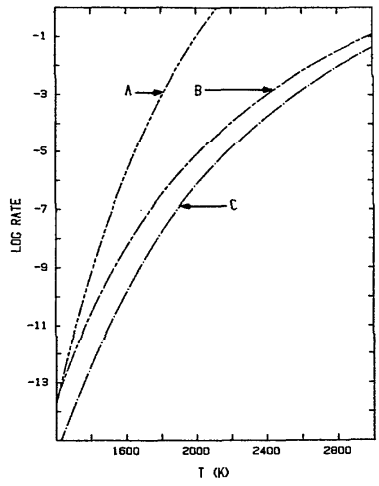

FIG. 16. SrO maximum vaporization rates. A—10^{-15} bar O_2; B—congruent vaporization; C—0.2 bar O_2.

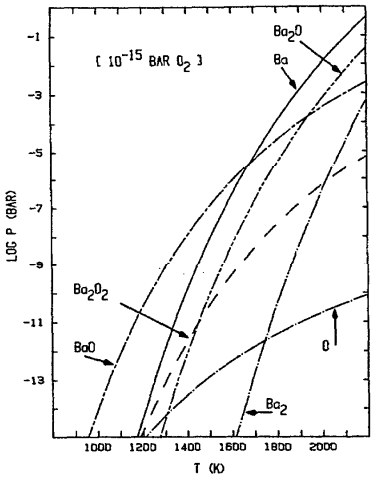

FIG. 17. BaO vaporization in 10^{-15} bar O_2.

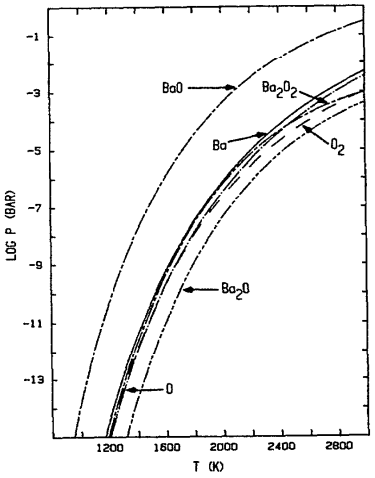

FIG. 18. BaO congruent vaporization.

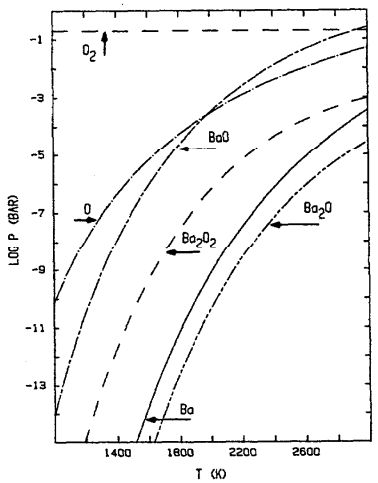

FIG. 19. BaO vaporization in 0.2 bar O_2.

law treatment of the equilibrium data of Drowart *et al.* (1964) using these calculated functions. As can be seen in the graphs, Sr_2O is a minor feature of the vaporization chemistry under each of the environmental conditions.

CaO_2(s) thermodynamic data—the enthalpy of formation was recalculated by (Garvin *et al.*, 1987) from the experimental data cited by Glushko *et al.* (1979b).

e. Ba–O System

BaO(s) is the condensed phase stable at high temperatures under neutral and reducing conditions. In oxidizing atmospheres BaO_2(s) is stable at low temperatures; the O_2 pressure over BaO_2(s) reaches 0.2 bar at about 1000 K (Vannerberg, 1962; Kedrovskii *et al.*, 1967).

The calculated vaporization equilibria shown in Figs. 17–19 indicate that BaO(g) is the principal product for vaporization under oxidizing and neutral conditions, but that Ba(g) becomes important at high temperatures under reducing conditions. It should be pointed out that our calculated neutral vapor composition differs appreciably from the reported results of four separate mass spectrometric studies (Inghram *et al.*, 1955; Newbury *et al.*, 1968; Semenov *et al.*, 1972; Hilpert and Gerads, 1975) in that the latter indicate almost comparable BaO and Ba partial pressures at 1500 to 1800 K. Recent mass spectrometric investigation in our own laboratory (Lamoreaux and Hildenbrand, 1983), however, show that under neutral conditions the ratio $p(BaO)/p(Ba) > 100$, so that, as suspected, some reduction of BaO was occurring in the earlier work. The calculated maximum vaporization rate is shown in Fig. 20.

Here again, the major compilations do not include data for the species Ba_2O_2 and Ba_2O, but they are included here for completeness since they have been observed; molecular constants were selected as noted below. The enthalpies of formation for these species were chosen so as to be consistent with the neutral composition inferred from our mass spectra at low ionizing energy.

Ba_2O(g) thermodynamic data—the Gibbs energy functions were calculated using the approximate molecular

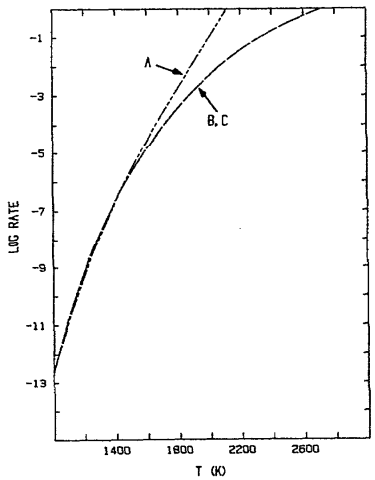

FIG. 20. BaO maximum vaporization rates. A—10^{-15} bar O_2; B—congruent vaporization; C—0.2 bar O_2.

constants of Kudin (1981): $r(\text{Ba–O}) = 0.231$ nm, $\angle\text{Ba–O–Ba} = 180°$, electronic ground state degeneracy = 3, no excited electronic states, and vibrational fundamentals of 500, 280(2), and 720 cm^{-1}.

Ba_2O_2 thermodynamic data—the Gibbs energy functions were calculated using the matrix isolation spectroscopy results of Ault and Andrews (1975) for the planar rhombic molecule with a derived O–Ba–O angle of 102° and observed vibrational fundamentals at 402 and 501 cm^{-1}, and the estimated molecular constants of Kudin (1981): $r(\text{Ba–O}) = 0.21$ nm, vibrational fundamentals 470, 330, 270, and 200 cm^{-1}, electronic ground state degeneracy = 1, and no excited electronic states.

f. B–O System

The stable solid phase is B_2O_3, with a melting point of 723 K. Vaporization takes place primarily by evolution of $B_2O_3(g)$, except that $B_2O_2(g)$ becomes important at high temperatures under reducing conditions and $BO_2(g)$ is important at low temperatures under oxidizing conditions. The calculated vaporization equilibria and vaporization rates are shown in Figs. 21–24. Partial pressures under reducing conditions were calculated for an O_2 partial pressure of 10^{-15} bar up to 1923 K, where the calculated O_2 pressure of the B–B_2O_3 equilibrium reaches this value, and for the O_2 pressure of the B–B_2O_3 equilibrium at higher temperatures. If liquid B_2O_3 is the only condensed phase present, its composition will change during vaporization unless $B_2O_3(g)$ evolution dominates; if the liquid composition is changing, the partial pressures indicated are thus strictly applicable only at the start of vaporization.

g. Al–O System

Al_2O_3 is the stable solid phase in this system. The major gaseous aluminum species are Al, AlO, and Al_2O, depending on conditions. Some earlier reviews selected data that indicated a much higher thermodynamic stability for $AlO_2(g)$, such that this species dominated the vaporization chemistry under oxidizing conditions. We agree with the recent

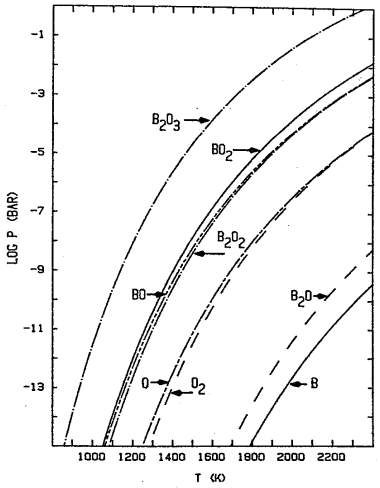

FIG. 22. B_2O_3 congruent vaporization.

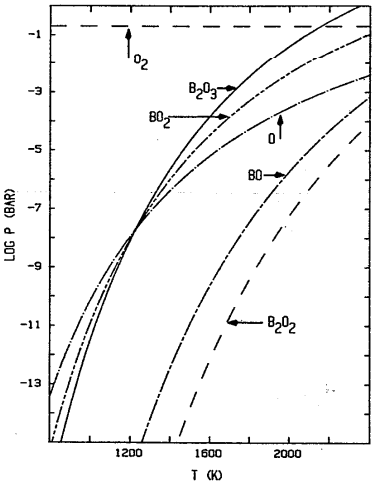

FIG. 23. B_2O_3 vaporization in 0.2 bar O_2.

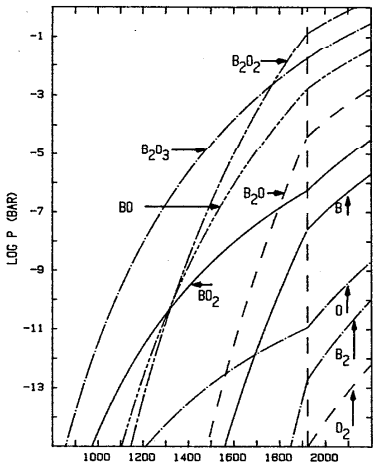

FIG. 21. B_2O_3 vaporization in 10^{-15} bar O_2 below 1923 K and vaporization of B–B_2O_3 mixture above 1923 K.

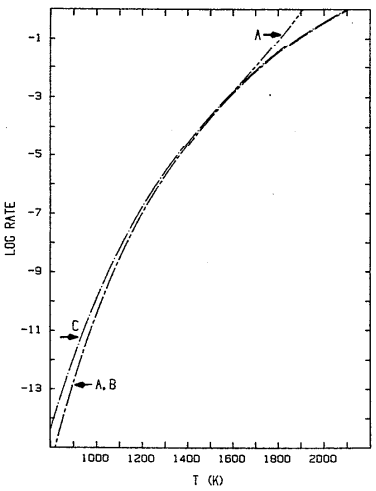

FIG. 24. B_2O_3 maximum vaporization rates. A—10^{-15} bar O_2; B—congruent vaporization; C—0.2 bar O_2.

IVTAN (Glushko *et al.*, 1981) and JANAF table (Stull *et al.*, 1971, December 31, 1979 unbound supplement) publications that assign a significantly lower stability to $AlO_2(g)$, based primarily on the studies of Ho and Burns (1980). The calculated vaporization equilibria and maximum vaporization rates are shown in Figs. 25–28. Vaporization under reducing conditions was calculated for an O_2 pressure of 10^{-15} bar of O_2 up to 2230 K, where the calculated O_2 pressure of the Al–Al_2O_3 equilibrium reaches 10^{-15} bar, and for the O_2 pressure of the Al–Al_2O_3 equilibrium above this temperature.

h. Ga–O System

The stable solid phase is Ga_2O_3. The calculated vaporization equilibria and maximum vaporization rates are shown in Figs. 29–32. Vaporization under reducing conditions was calculated for an O_2 pressure of 10^{-15} bar up to 1446 K, where the O_2 pressure of the Ga–Ga_2O_3 equilibrium reaches this value, and for the O_2 pressure of the Ga–Ga_2O_3 equilibrium at higher temperatures.

i. In–O System

The stable solid phase is In_2O_3. The calculated vaporization partial pressures and maximum vaporization rates are shown in Figs. 33–36. Partial pressures under reducing conditions were calculated for an O_2 pressure of 10^{-15} bar up to 1239 K, where the O_2 pressure of the In–In_2O_3 equilibrium reaches this value, and for the O_2 pressure of the In–In_2O_3 equilibrium at higher temperatures.

j. Tl–O System

The stable solid oxide phase under neutral and reducing conditions, and in 0.2 atm of O_2 above about 1060 K, is Tl_2O. Tl_2O_3 is the stable phase at lower temperatures under oxidizing conditions. Calculated partial pressures and maximum rates for vaporization processes are shown in Figs. 37–40. Partial pressures over Tl_2O under reducing conditions were calculated for an O_2 pressure of 10^{-15} bar up to 731 K, where the O_2 partial pressure of the Tl–Tl_2O equilibrium

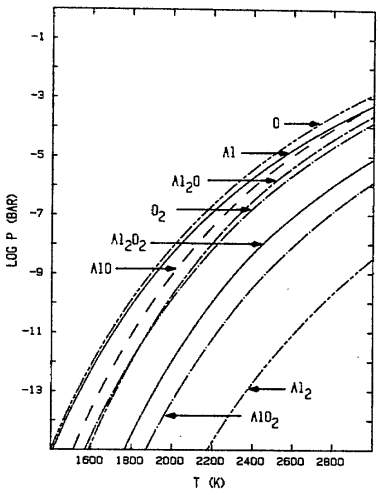

FIG. 26. Al_2O_3 congruent vaporization.

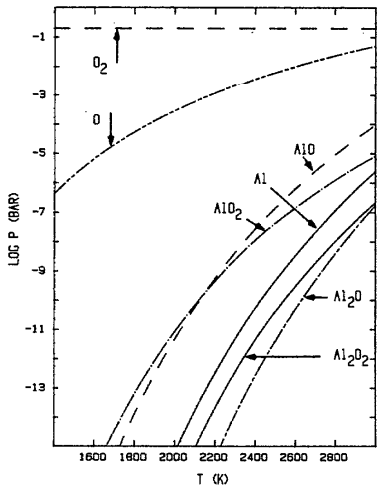

FIG. 27. Al_2O_3 vaporization in 0.2 bar O_2.

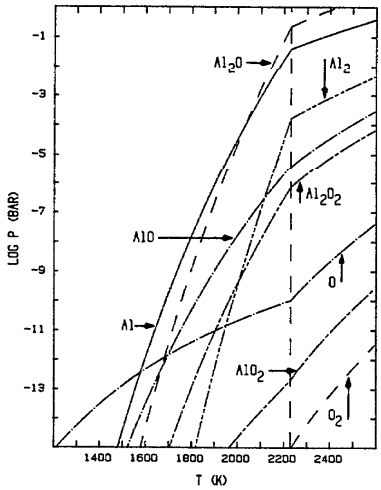

FIG. 25. Al_2O_3 vaporization in 10^{-15} bar O_2 below 2230 K and vaporization of Al–Al_2O_3 mixture above 2230 K.

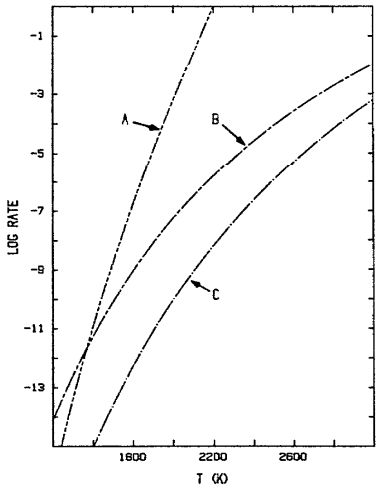

FIG. 28. Al_2O_3 maximum vaporization rates. A—10^{-15} bar O_2; B—congruent vaporization; C—0.2 bar O_2.

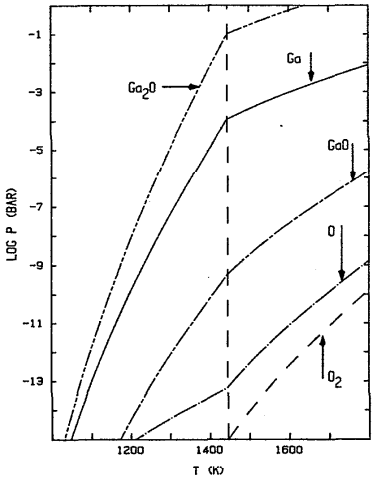

FIG. 29. Ga_2O_3 vaporization in 10^{-15} bar O_2 below 1446 K and vaporization of Ga–Ga_2O_3 mixture above 1446 K.

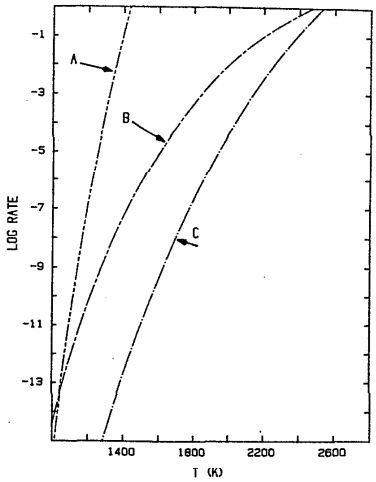

FIG. 32. Ga_2O_3 maximum vaporization rates. A—10^{-15} bar O_2; B—congruent vaporization; C—0.2 bar O_2.

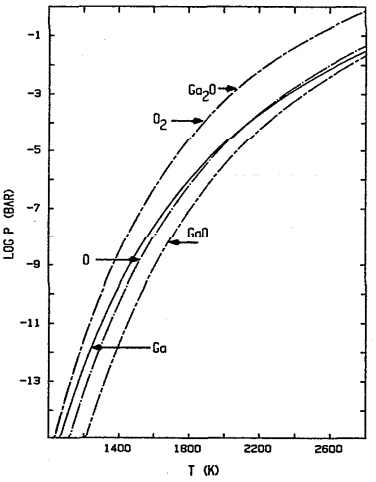

FIG. 30. Ga_2O_3 congruent vaporization.

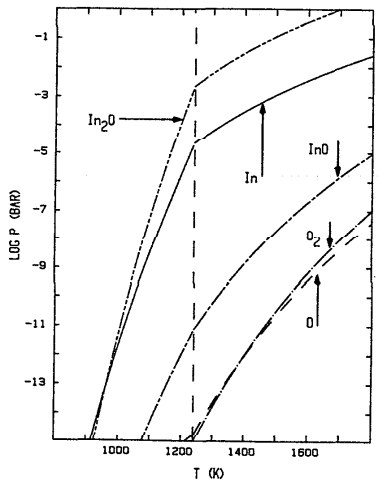

FIG. 33. In_2O_3 vaporization in 10^{-15} bar O_2 below 1239 K and vaporization of In–In_2O_3 mixture above 1239 K.

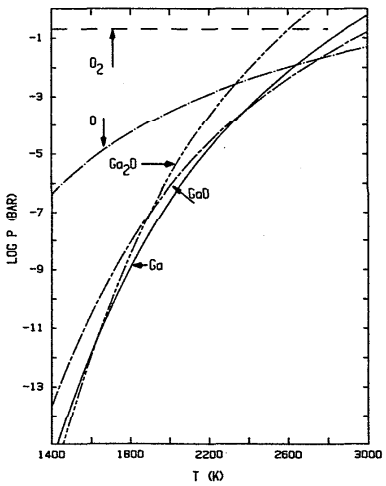

FIG. 31. Ga_2O_3 vaporization in 0.2 bar O_2.

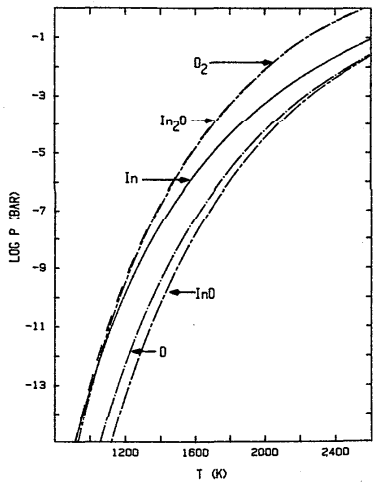

FIG. 34. In_2O_3 congruent vaporization.

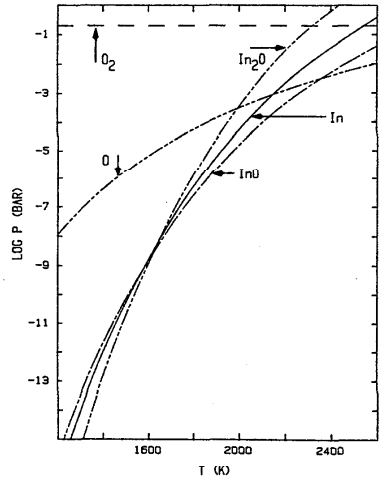

FIG. 35. In_2O_3 vaporization in 0.2 bar O_2.

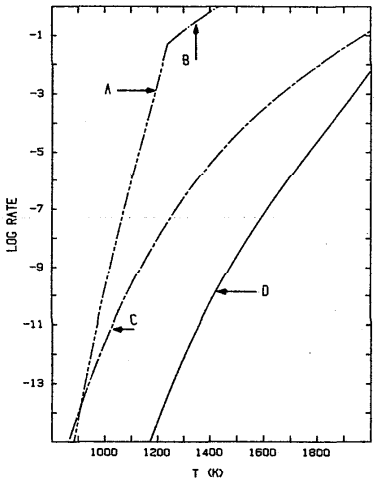

FIG. 36. In_2O_3 maximum vaporization rates. A—10^{-15} bar O_2; B—In–In_2O_3; C—congruent vaporization; D—0.2 bar O_2.

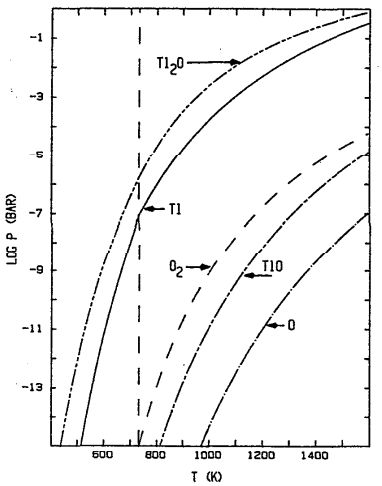

FIG. 37. Tl_2O vaporization in 10^{-15} bar O_2 below 731 K and vaporization of Tl–Tl_2O mixture above 731 K.

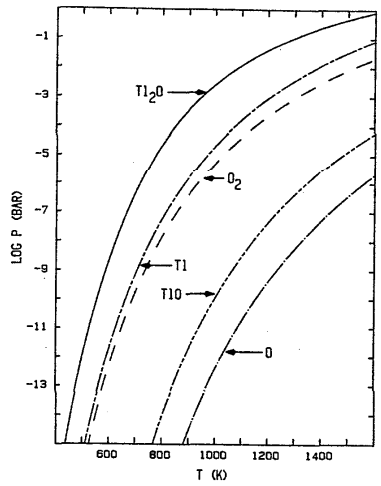

FIG. 38. Tl_2O congruent vaporization.

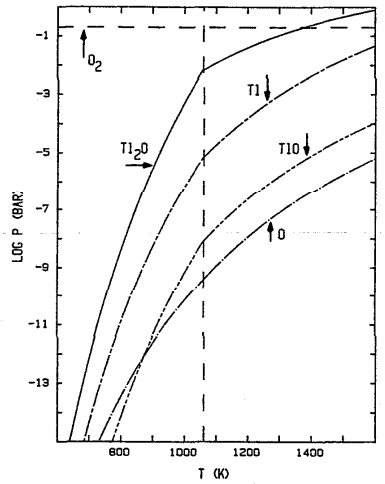

FIG. 39. Tl_2O_3 vaporization below 1060 K and TlO vaporization above 1060 K in 0.2 bar O_2.

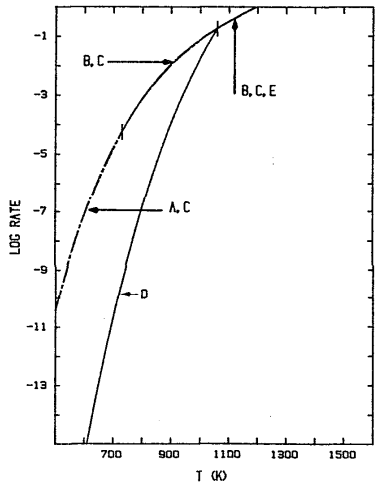

FIG. 40. Maximum vaporization rates of thallium oxides. A—Tl_2O in 10^{-15} bar O_2; B—Tl–Tl_2O equilibrium vaporization; C—Tl_2O congruent vaporization; D—Tl_2O_3 vaporization in 0.2 bar O_2; E—Tl_2O vaporization in 0.2 bar O_2.

reaches this value, and for the O_2 pressure of the Tl–Tl_2O equilibrium at higher temperatures. Partial pressures for vaporization in 0.2 bar of O_2 were calculated for Tl_2O_3 up to 1060 K, and for Tl_2O at higher temperatures.

k. Si–O System

Calculated partial pressures for vaporization of SiO_2 are shown in Figs. 41–44. SiO(g) is the principal silicon-containing vaporization product under neutral and reducing conditions, while SiO_2(g) is favored under oxidizing conditions below about 2500 K.

SiO_2 (quartz, cristobalite, liquid) thermodynamic data—the CODATA (Cox, 1978) value of the enthalpy of formation of quartz was accepted. Other data were taken from the recent article of Richet *et al.* (1982), which reviewed the available literature.

Si_2O_2(g) thermodynamic data—Gibbs energy functions were calculated using the molecular constants of Khanna *et al.* (1981) for a planar Si–O–Si–O molecule with the terminal atoms lying on opposite sides of the central O–Si bond axis: ∠Si–O–Si = ∠O–Si–O = 109.5°, r(Si–O, terminal) = 0.174 nm, r(Si–O, central) = 0.151 nm, ground electronic state degeneracy = 1, and no excited electronic states. The vibrational fundamentals as measured by infrared and Raman matrix isolation spectroscopy were 1222, 804, 766, 252, and 79 cm^{-1}; the remaining fundamental at 180 cm^{-1} was calculated by force constant calculations (Khanna *et al.*, 1981). The Gibbs energy functions calculated using these constants are 2.8 K greater than those calculated using the data of Anderson and Ogden (1969) for a molecule with D_{2h} symmetry. The enthalpy of formation was then calculated by the third-law method from the mass spectrometric data of Porter *et al.* (1955) and of Zmbov *et al.* (1973).

l. Ge–O System

The stable condensed phase below 1308 K is tetragonal GeO_2; the hexagonal crystal structure is stable from 1308 K to the melting temperature, 1388 K (Glushko *et al.*, 1979a). Calculated partial pressures for vaporization of GeO_2 are shown in Figs. 45–48. GeO is the major germanium-contain-

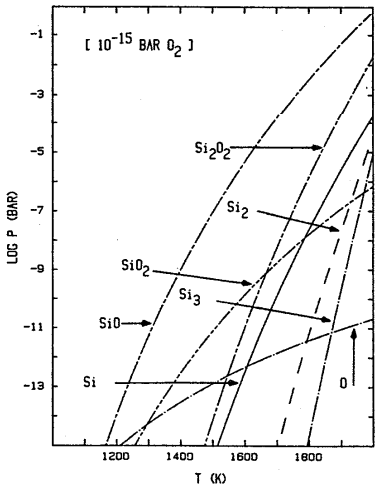

FIG. 41. SiO_2 vaporization in 10^{-15} bar O_2.

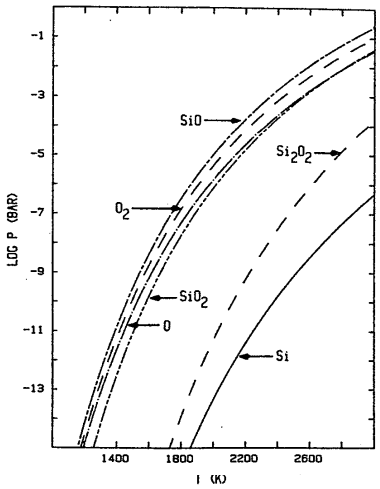

FIG. 42. SiO_2 congruent vaporization.

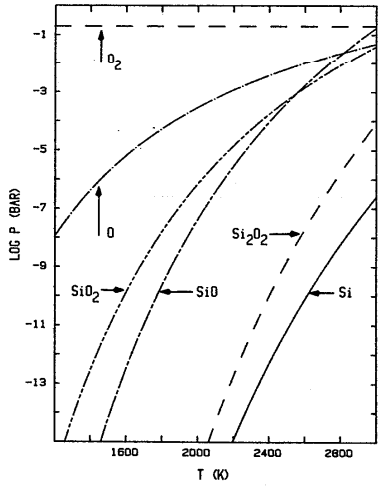

FIG. 43. SiO_2 vaporization in 0.2 bar O_2.

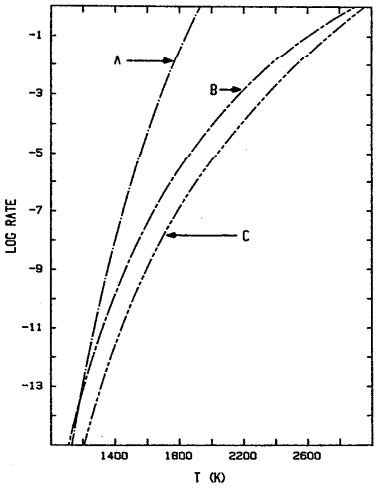

FIG. 44. SiO_2 maximum vaporization rates. A—10^{-15} bar O_2; B—congruent vaporization; C—0.2 bar O_2.

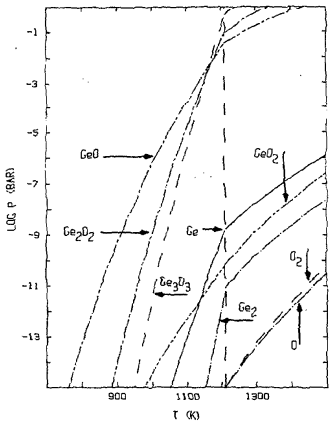

FIG. 45. GeO_2 vaporization in 10^{-15} bar O_2 below 1210 K and vaporization of Ge–GeO_2 mixture above 1210 K.

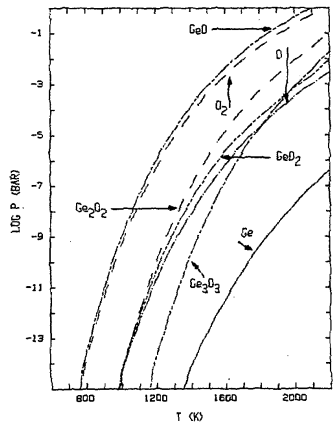

FIG. 46. GeO_2 congruent vaporization.

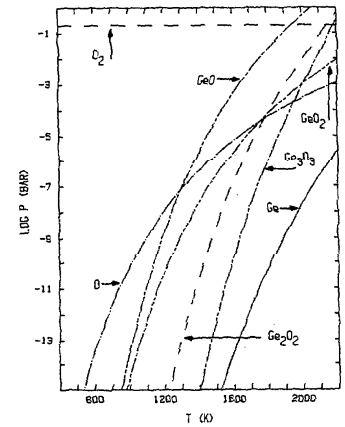

FIG. 47. GeO_2 vaporization in 0.2 bar O_2.

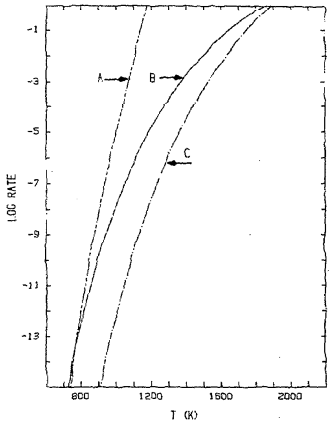

FIG. 48. GeO_2 maximum vaporization rates. A—10^{-15} bar O_2; B—congruent vaporization; C—0.2 bar O_2.

ing vapor species under most conditions, with the polymeric species Ge_2O_2 and Ge_3O_3 becoming important at higher temperatures under reducing conditions.

$Ge_2O_2(g)$ thermodynamic data—Gibbs energy functions were calculated using the molecular data of Ogden and Ricks (1970) which were estimated except for the observed vibrational fundamentals at 601 and 666 cm^{-1}: D_{2h} symmetry, symmetry number = 4, $r(Ge–O) = 0.187$ nm, ∠O–Ge–O = 83°. The electronic ground state degeneracy was taken as unity, no excited electronic states were considered, and the remaining vibrational fundamentals of 120, 500, 450, and 80 cm^{-1} were estimated by analogy with the alkali metal M_2O_2 species (Lamoreaux and Hildenbrand, 1984). The enthalpy of vaporization was chosen to yield calculated vaporization equilibria consistent with the mass spectrometric data of Drowart *et al.* (1965).

$Ge_3O_3(g)$ thermodynamic data—Gibbs energy functions were calculated using the molecular data of Ogden and Ricks (1970), which were estimated except for doubly degenerate vibrational fundamentals at 824 and 438 cm^{-1}: D_{3h} symmetry, symmetry number = 6, $r(Ge–O) = 0.185$ nm, ∠O–Ge–O = 100°, ∠Ge–O–Ge = 140°. The electronic ground state degeneracy was taken to be 1, no excited electronic states were considered, and the remaining vibrational fundamentals were estimated by analogy to Be_3O_3: 159(2), 70(2), 150, 70(2), and 90 cm^{-1}. The enthalpy of formation was chosen to yield calculated vaporization equilibria in agreement with the mass spectrometric studies of Drowart *et al.* (1965).

m. Sn–O System

The stable condensed phase is SnO_2. Calculated partial pressures for vaporization of SnO_2 are shown in Figs. 49–52. SnO(g) is the principal tin-containing vaporization species, with the polymeric species Sn_2O_2, Sn_3O_3, and Sn_4O_4 becoming important at higher temperatures under reducing conditions.

$Sn_2O_2(g)$ thermodynamic data—because the existing spectroscopic data are insufficient to adequately determine

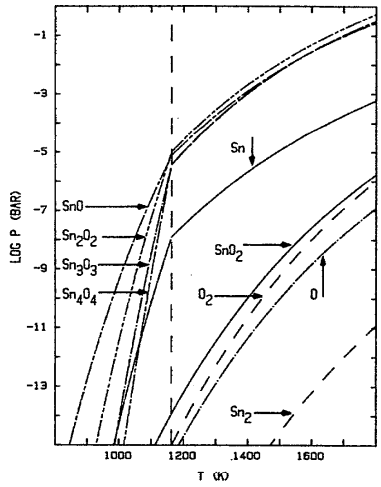

FIG. 49. SnO_2 vaporization in 10^{-15} bar O_2 below 1163 K and vaporization of Sn–SnO_2 mixture above 1163 K.

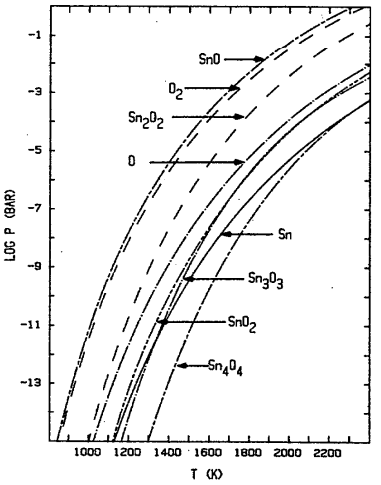

FIG. 50. SnO_2 congruent vaporization.

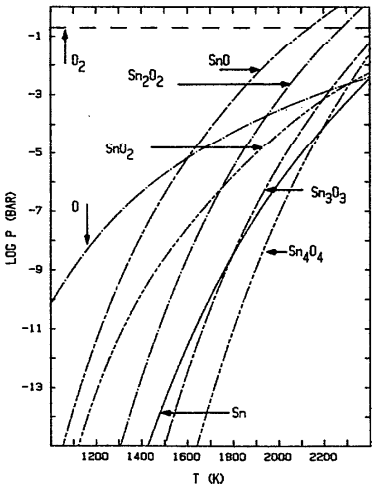

FIG. 51. SnO_2 vaporization in 0.2 bar O_2.

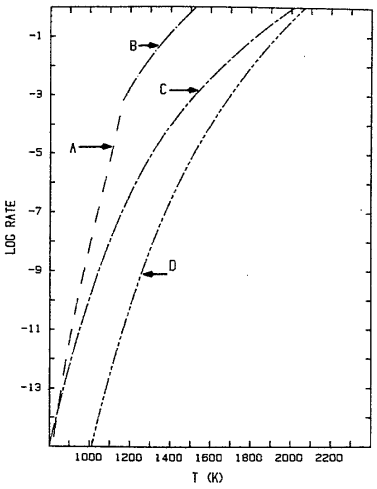

FIG. 52. SnO_2 maximum vaporization rates. A—10^{-15} bar O_2; B—Sn–SnO_2 equilibrium; C—congruent vaporization; D—0.2 bar O_2.

the molecular constants of $Sn_2O_2(g)$, the estimated S°_{298}/R value of Colin *et al.* (1965) was used along with the estimated value $C^\circ_p/R = 2.3$ g-at. derived by analogy to other gaseous compounds to calculate the Gibbs energy functions shown in Table 2. The enthalpy of formation was selected to yield calculated equilibria in agreement with the results of Colin *et al.*; the thermodynamic data presented in Tables 2 and 3 are consistent with observed partial pressures over the temperature range of the mass spectrometer studies.

$Sn_3O_3(g)$ thermodynamic data—the data were derived as for $Sn_2O_2(g)$, except that the value of C°_p/R was estimated as 2.5/g-at.

$Sn_4O_4(g)$ thermodynamic data—the data were derived as for $Sn_3O_3(g)$.

n. Pb–O System

The stable condensed oxide phase under neutral and reducing conditions, and in 0.2 atm of O_2 at temperatures above about 800 K, is PbO. Calculated partial pressures for vaporization of PbO are shown in Figs. 53–56. The predominant vapor phase species under neutral and oxidizing conditions are PbO and its polymers Pb_2O_2, Pb_3O_3, Pb_4O_4, Pb_5O_5, and Pb_6O_6; under reducing conditions the predominant vapor species is atomic lead.

Pb_2O_2, Pb_3O_3, Pb_4O_4, Pb_5O_5, and Pb_6O_6 thermodynamic data—Drowart, Colin, and Exsteen (1965) and Kazenas, Chizhikov, and Tsvetkov (1968) analyzed the vapors over PbO by mass spectroscopy. The thermodynamic properties of the gaseous PbO polymers given in Tables 2 and 3 were derived from the results of Drowart and co-workers, who made measurements to 1200 K and observed all five of these species. Kazenas *et al.* made measurements at temperatures up to 950 K and did not observe the pentamer or hexamer. The enthalpies of formation and entropies at 298 K selected by Drowart *et al.* were accepted for the dimer, trimer, and tetramer; the Gibbs energy functions for these species were derived by assuming that $C^\circ_p/R = 3.0$/g-at. at all temperatures above 298 K. Although this heat capacity

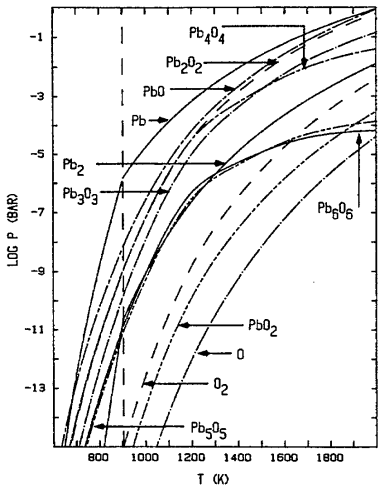

FIG. 53. PbO vaporization in 10^{-15} bar O_2 below 905 K and vaporization of Pb–PbO mixture above 905 K.

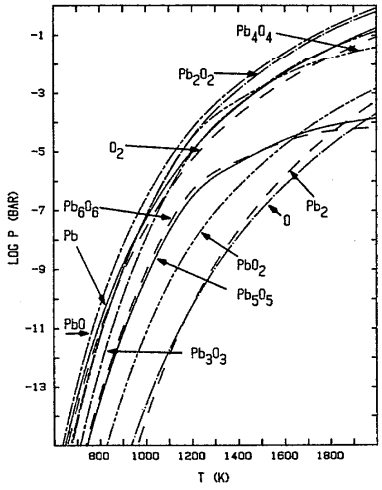

FIG. 54. PbO congruent vaporization.

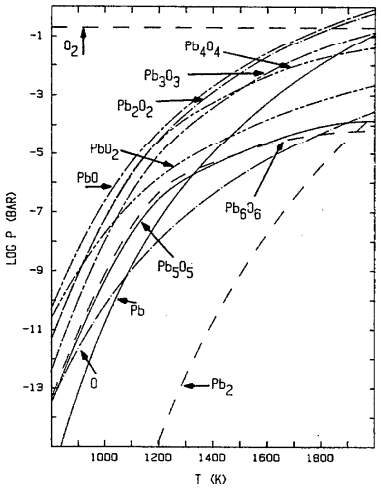

FIG. 55. PbO vaporization in 0.2 bar O_2.

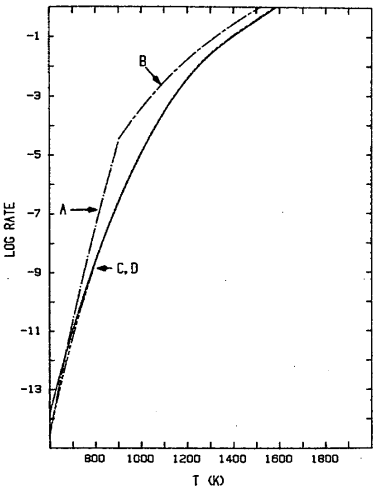

FIG. 56. PbO maximum vaporization rates. A—10^{-15} bar O_2; B—Pb–PbO equilibrium; C—congruent vaporization; D—0.2 bar O_2.

value seems somewhat large, calculations using the resulting thermodynamic properties are in excellent agreement with Drowart's gas phase equilibria over the temperature range of measurements. Equilibrium data are available for Pb_5O_5 and Pb_6O_6 at only one temperature, 1200 K. The entropy at 298 K for these two species was estimated by extrapolating the values for the monomeric through tetrameric species, and the estimated value $C_p^\circ/R = 3.0$ was used to calculate values of the Gibbs energy functions. The gas phase equilibria at 1200 K were then used to derive values of the enthalpies of formation.

o. Zn–O System

The stable solid phase is ZnO. Vaporization takes place predominantly by dissociation into gaseous Zn and O_2, and a much smaller amount of ZnO(g). Figures 57–60 show calculated partial pressures for vaporization of ZnO. The Gibbs energy function of gaseous ZnO was calculated using the estimated internuclear distance of Brewer and Rosenb-

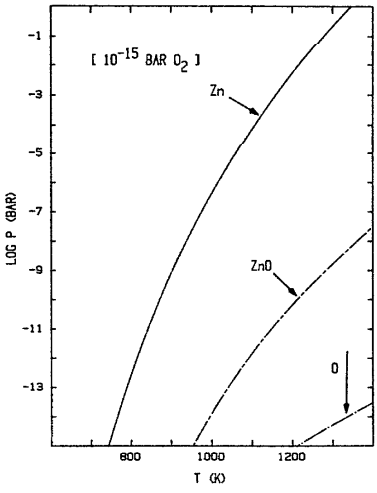

FIG. 57. ZnO vaporization in 10^{-15} bar O_2.

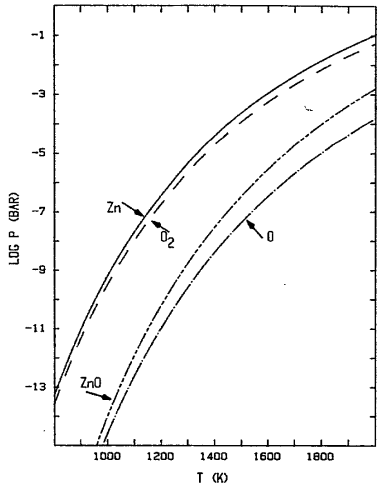

FIG. 58. ZnO congruent vaporization.

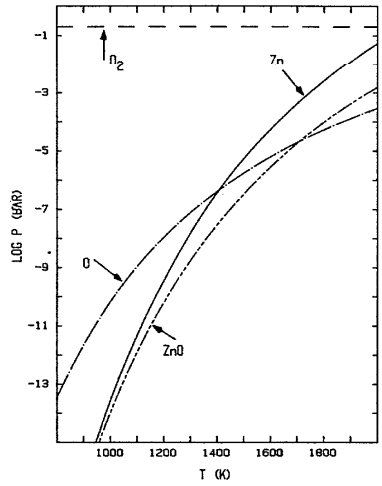

FIG. 59. ZnO vaporization in 0.2 bar O_2.

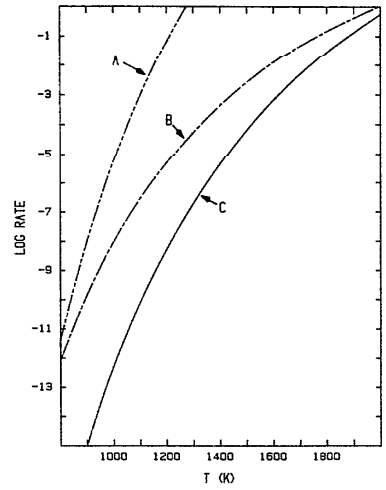

FIG. 60. ZnO maximum vaporization rates. A—10^{-15} bar O_2; B—congruent vaporization; C—0.2 bar O_2.

latt (1969) for the nondegenerate electronic ground state, r(Zn–O) = 0.174 nm and the value of the vibrational fundamental, 810 cm^{-1}, from the matrix-isolation study of Prochaska and Andrews (1980). The selected value of $\Delta_f H^\circ_{298}/R$ for ZnO(g), 10.9 ± 1 kK, was derived using the mass spectrometric relative intensity measurements of Grade *et al.* (1982) for the vaporization of ZnO(s), and is in reasonable accord with the selected value of Pedley and Marshall (1983), 13.1 ± 5 kK.

p. Cd–O System

The stable solid phase is CdO. Vaporization takes place predominantly by dissociation into gaseous Cd and O_2 and a much smaller amount of CdO(g). Figures 61–64 show calculated partial pressures for vaporization of CdO. The Gibbs energy function of CdO(g) was calculated using the estimated internuclear distance of Brewer and Rosenblatt (1969) for the nondegenerate electronic ground state, r(Cd–O) = 0.185 nm. The vibrational fundamental, 719 cm^{-1}, was taken from the matrix-isolation study of Prochaska and Andrews (1980). The selected value of $\Delta_f H^\circ_{298}/R$ for CdO(g), 15.6 ± 1 kK, was derived from the mass spectrometric relative intensity measurements of Grade and Hirschwald (1982) for the vaporization of CdO(s), and is in good accord with the selected value of Pedley and Marshall (1983), 15.1 ± 10 kK, and the lower limit found by Behrens and Mason (1981), 13.7 kK.

q. Hg–O System

The stable solid phase is HgO. Vaporization takes place primarily by dissociation into gaseous Hg and O_2 and a smaller amount of HgO(g). Figures 65–68 show calculated partial pressures for vaporization of HgO. The Gibbs energy function of HgO(g) was calculated using the estimated internuclear distance of Brewer and Rosenblatt (1969), 0.195 nm, for the nondegenerate electronic ground state and the vibrational fundamental, 676 cm^{-1}, of Butler *et al.* (1979) determined by matrix-isolation spectroscopy. The calculated values of $-(G^\circ_T - H^\circ_{298})/RT$ are about 0.1 greater

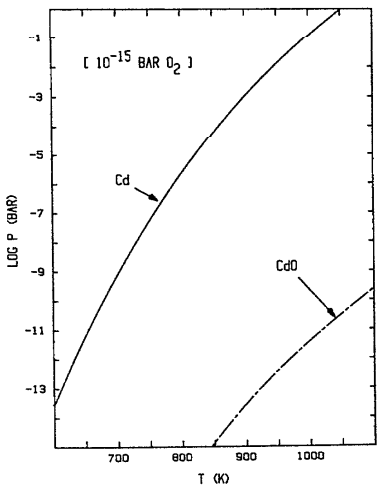

FIG. 61. CdO vaporization in 10^{-15} bar O_2.

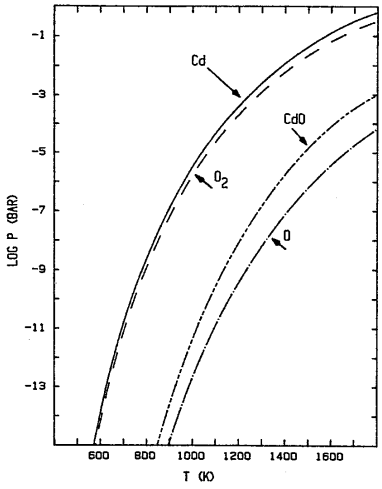

FIG. 62. CdO congruent vaporization.

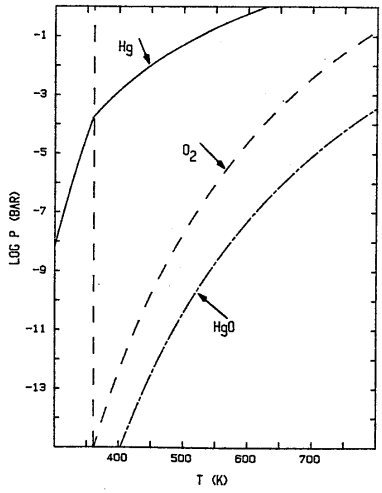

FIG. 65. HgO vaporization in 10^{-15} bar O_2 below 361 K and vaporization of Hg–HgO mixture above 361 K.

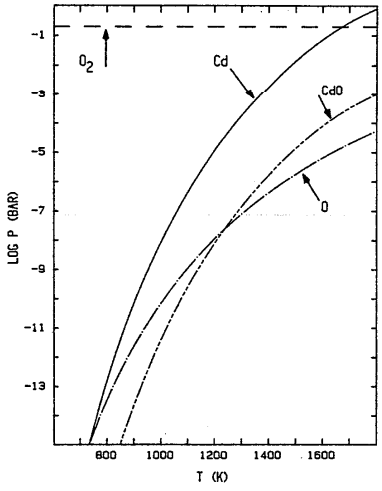

FIG. 63. CdO vaporization in 0.2 bar O_2.

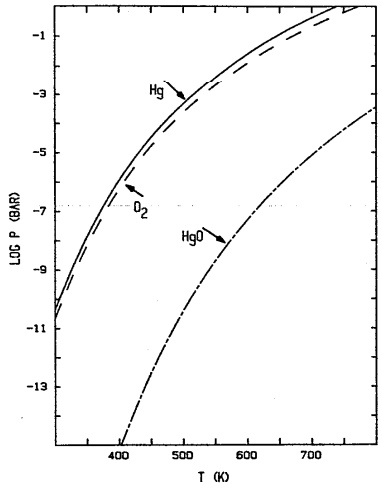

FIG. 66. HgO congruent vaporization.

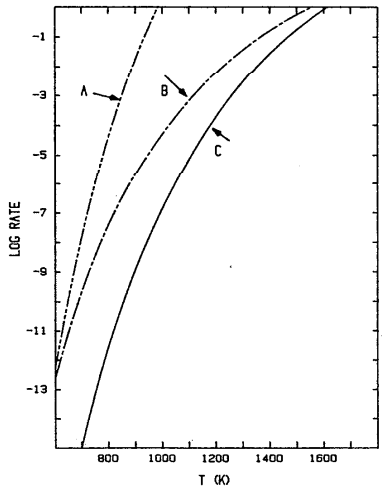

FIG. 64. CdO maximum vaporization rates. A—10^{-15} bar O_2; B—congruent vaporization; C—0.2 bar O_2.

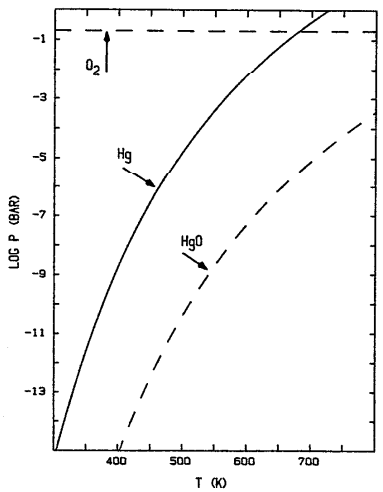

FIG. 67. HgO vaporization in 0.2 bar O_2.

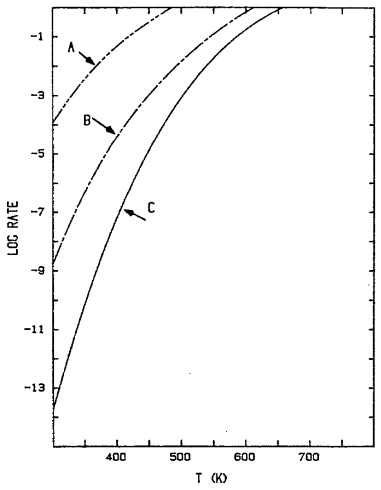

FIG. 68. HgO maximum vaporization rates. A—10^{-15} bar O_2; B—congruent vaporization; C—0.2 bar O_2.

than those of JANAF (Stull *et al.*, 1971) from 298 to 2000 K. The selected value of $\Delta_f H^\circ_{298}/R$ for HgO(g), 11.2 ± 1 kK, was derived from the mass spectrometric ion intensity ratio measurements of Grade and Hirschwald (1982). JANAF (Stull *et al.*, 1971), and Pankratz (1982) had selected the estimated value 5 ± 8 kK.

3. High-Temperature Equilibria and Reaction Rates

Calculations using the selected thermochemical data were discussed in the previous paper (Lamoreaux and Hildenbrand, 1984). The basic equations are presented here so that species partial pressures and maximum vaporization rates can be calculated for specific temperatures and oxidation conditions.

3.1. Mathematics of Vaporization Calculations

For many vaporization conditions one or two vapor species are predominant, and calculation of the chemical equilibrium from thermodynamic data is straightforward. Calculations can be more complicated when several species are present in significant quantities. The following procedure is a general method for calculating the equilibrium pressures of vapor species in equilibrium with a condensed phase of known composition.

The chemical species present at equilibrium in the vaporization of a condensed binary oxide can be described mathematically as being formed by linear combination of the vaporizing oxide M_bO_c and oxygen O_2 according to the general reaction for the production of species i,

$$d(\mathrm{i})M_bO_c(\mathrm{s,l}) + e(\mathrm{i})O_2(\mathrm{g}) = M_{x(\mathrm{i})}O_{y(\mathrm{i})}(\mathrm{s,l,\ or\ g}), \quad (2)$$

where $e(\mathrm{i})$ may be zero, negative, or positive. Possible species include the vaporizing phase M_bO_c (s or l), considered to be species 1, and O_2(g) as well as the species produced by their linear combination. From mass balance,

$$d(\mathrm{i}) = x(\mathrm{i})/b \quad (3)$$

and

$$e(\mathrm{i}) = [by(\mathrm{i}) - cx(\mathrm{i})]/2b. \quad (4)$$

We define the Gibbs energy of species i at temperature T as

$$G^\circ_T(\mathrm{i})/RT = (G^\circ_T - H^\circ_{298})/RT + \Delta_f H^\circ_{298}(\mathrm{i})/RT. \quad (5)$$

The Gibbs energy change for the reaction producing species i from M_bO_c (s or l) and O_2(g), $\Delta_r G^\circ_T(\mathrm{i})$, is given by

$$\Delta_r G^\circ_T(\mathrm{i})/RT = G^\circ_T(\mathrm{i})/RT - d(\mathrm{i}) \times G^\circ_T[M_bO_c(\mathrm{s\ or\ l})]/RT - e(\mathrm{i})G^\circ_T[O_2(\mathrm{g})]/RT, \quad (6)$$

and the equilibrium constant for producing gas species i is

$$K(\mathrm{i}) = \exp[-\Delta_r G^\circ_T(\mathrm{i})/RT] = p(\mathrm{i})/\{a(1)^{d(\mathrm{i})}p[O_2(\mathrm{g})]^{e(\mathrm{i})}\}, \quad (7)$$

where the pressures $p(\mathrm{i})$ are considered low enough that they are equal to fugacities, and a (1) is the activity of M_bO_c. If M_bO_c is a pure condensed phase, its activity is unity, and

$$p(\mathrm{i}) = k(\mathrm{i})p(O_2)^{e(\mathrm{i})} \quad (8)$$

for the gas species. If the oxygen pressure is known, the pressure of each species i can be calculated from this equation.

For congruent vaporization, the vapor composition is the same as the condensed phase, and

$$\frac{\Sigma[p(\mathrm{i})x(\mathrm{i})]}{\Sigma[p(\mathrm{i})y(\mathrm{i})]} = \frac{b}{c}. \quad (9)$$

This leads to the expression

$$\sum\{K(\mathrm{i})p(O_2)^{e(\mathrm{i})}[cx(\mathrm{i}) - by(\mathrm{i})]\} = 0, \quad (10)$$

where summation is over the gaseous species present. In practice, this equation is solved for $p(O_2)$ by graphical interpolation or by numerical methods. The value found for $p(O_2)$ is then used in Eq. (8) to find the other partial pressures.

For the above calculations to correspond to equilibrium vaporization, they must be used for vaporization of the condensed oxide phases or phases stable under the particular vaporization conditions. Where more than one oxide phase is a possibility, the stable phase or phases must be determined. Two condensed oxide phases of fixed composition at a given temperature are related by the equilibrium

$$\mathrm{Oxide(1)} = \mathrm{Oxide(2)} + fO_2(\mathrm{g}). \quad (11)$$

Oxide(1) is assumed to have the greater oxygen activity. The equilibrium constant for this reaction is

$$K_{eq} = a(2)p(O_2)^f/a(1). \quad (12)$$

If both condensed phases are at equilibrium, their activities are unity, and the pressure of O_2 is given by the equation

$$p_{eq}(O_2) = K_{eq}^{(1/f)}. \quad (13)$$

Oxide (1) is the stable phase for O_2 pressures greater than $p_{eq}(O_2)$, and oxide (2) is stable for O_2 pressures less than $p_{eq}(O_2)$ at the given temperature.

3.2. Vaporization Rate Calculations

Maximum vaporization rates are calculated using the Hertz–Knudsen equation of classical kinetic theory, which applies to free vaporization from an uncontaminated surface at low pressures. For gas species i evolving from the surface, the maximum vaporization rate $dn(i)/dt$ in mol cm^{-2} s^{-1} is

$$\frac{dn(i)}{dt} = \frac{p(i)}{[2\pi M(i)RT]^{1/2}}, \quad (14)$$

where $M(i)$ and $p(i)$ are the gram molecular weight and equilibrium partial pressure of vapor species i, and R and T are the molar gas constant and absolute temperature. Since 1 bar is 10^6 dyn cm^{-2} and R is 8.3144×10^6 erg mol^{-1} deg^{-1}, for pressures in bar, this is equivalent to

$$\frac{dn(i)}{dt} = 43.8\left(\frac{p(i)}{[M(i)T]^{1/2}}\right) \text{mol cm}^{-2}\,\text{s}^{-1}. \quad (15)$$

Calculation of maximum vaporization rates is more difficult for incongruent than for congruent processes. In general, solid-phase activities during the vaporization process are not known, and calculated maximum vaporization rates of oxides that deviate from their original stoichiometry should be considered indicative rather than exact (Beruto *et al.*, 1981). In the present work, maximum vaporization rates have been calculated for incongruent, as well as congruent vaporization. Only initial vaporization rates, for which no condensed phase composition changes have taken place, are considered. Vaporization rates are expressed in terms of the mass of originally present oxide M_bO_c lost as measured by the volatility of metal atoms. The total mass loss thus calculated is

$$\frac{dm}{dt} = 44.3\left(\frac{M(M_bO_c)}{b}\right)\sum\left(\frac{p(i)x(i)}{[M(i)T]^{1/2}}\right), \quad (16)$$

where dm/dt is the mass loss rate in g cm^{-2} s^{-1}, M_bO_c is the formula of the condensed oxide, and $x(i)$ and $M(i)$ are the number of gram atoms of metal per mole and gram molecular weight of gas species i.

Although actual vaporization rates may be lower because of kinetic factors, the calculated maximum vaporization rate is useful as a rough guide to material loss rates. Recent references on maximum vaporization rates include works by Turkdogan (1980) and Beruto *et al.* (1981).

4. Acknowledgments

We thank Susie Hahn and Gilbert Tong for their assistance. Financial support for this work has come from the Office of Standard Reference Data of the National Bureau of Standards under Grant NB80NADA1063.

5. References

Ackermann, R. J., and Thorn, R. J. (**1961**). *Progress in Ceramic Science* (Pergamon, New York), Vol. 1, p. 39.

Amitin, E. B., Minenkov, Yu. F., Nabutovskaya, O. A., Paukov, I. E., and Solokova, S. I. (**1984**). J. Chem. Thermodyn. **16**, 431.

Anderson, J. S., and Ogden, J. S. (**1969**). J. Chem. Phys. **51**, 4189.

Ault, B. S., and Andrews, L. (**1975**). J. Chem. Phys. **62**, 2312.

Balasubramanian, K., and Pitzer, K. S. (**1983**). J. Chem. Phys. **78**, 321; see also (**1984**) J. Chem. Phys. **80**, 592.

Barin, I., and Knacke, O. (**1973**). *Thermochemical Properties of Inorganic Substances* (Springer, Berlin); see also Supplement (1977).

Behrens, R. G., and Mason, C. F. (**1981**). J. Less-Common Metals. **77**, 169.

Beruto, D., Barco, L., and Passerone, A. (**1981**). "Refractory Oxides: High Temperature Gas–Solid and Solid–Liquid Behavior," in *Oxides and Oxide Films*, edited by A. K. Vijh (Dekker, New York), Vol. 6, pp. 1–84.

Brewer, L. (**1953**). Chem. Rev. **52**, 1.

Brewer, L. (**1977**). "The Cohesive Energies of the Elements," Lawrence Berkeley Laboratory Report LBL-3720.

Brewer, L. (**1983**). University of California, Berkeley, California, unpublished work.

Brewer, L. (**1984**). High Temp. Sci. **17**, 1.

Brewer, L., and Rosenblatt, G. (**1961**). Chem. Rev. **61**, 257.

Brewer, L., and Rosenblatt, G. M. (**1969**). *Advances in High Temperature Chemistry* (Academic, New York), Vol. 2, p. 1.

Butler, R., Katz, S., Snelson, A., and Stephens, J. B. (**1979**). J. Phys. Chem. **83**, 2578.

Chase, M. W. *et al.* (Eds.) (**1974**). JANAF Thermochemical Tables, 1974 Supplement, J. Phys. Chem. Ref. Data **3**, 311.

Chase, M. W. *et al.* (Eds.) (**1975**). JANAF Thermochemical Tables, 1975 Supplement, J. Phys. Chem. Ref. Data **4**, 1.

Chase, M. W. *et al.* (Eds.) (**1978**). JANAF Thermochemical Tables, 1978 Supplement, J. Phys. Chem. Ref. Data **7**, 793.

Chase, M. W. *et al.* (Eds.) (**1982**). JANAF Thermochemical Tables, 1982 Supplement, J. Phys. Chem. Ref. Data **11**, 695.

Chase, M. W. *et al.* (Eds.) (**1985**). JANAF Thermochemical Tables, 3rd ed., J. Phys. Chem. Ref. Data **14**, Supplement 1.

Chupka, W. A., Berkowitz, J., and Giese, C. F. (**1959**). J. Chem. Phys. **30**, 827.

Cox, J. D. (**1978**). J. Chem. Thermodyn. **10**, 903.

Colin, R., Drowart, J., and Verhaegen, G. (**1965**). Trans. Faraday Soc. **61**, 1364.

Coughlin, J. P. (**1954**). U.S. Bur. Mines Bull. **542**.

Desai, P. D. (**1986a**). J. Phys. Chem. Ref. Data. **15**, 967.

Desai, P. D. (**1986b**). Presentation at the 10th International CODATA Conference, Ottawa, Canada and subsequent private communication.

Drowart, J., Colin, R., and Exsteen, G. (**1965**). Trans. Faraday Soc. **61**, 1376.

Drowart, J., Degreve, F., Verhaegen, G., and Colin, R. (**1965**). Trans. Faraday Soc. **61**, 1072.

Drowart, J., Exsteen, G., and Verhaegen, G. (**1964**). Trans. Faraday Soc. **60**, 1920.

Garvin, D., Parker V. B., and White, Jr., H. J. (Eds.), *CODATA Thermodynamic Tables: Selections for Some Compounds of Calcium and Related Mixtures* (Hemisphere, New York, 1987).

Glushko, V. P., Gurvich, L. V., Bergman, G. A., Veitz, I. V., Medvedev, V. A., Khachkuruzov, G. A., and Yungman, V. S. (**1978**). *Thermodynamic Data for Individual Substances* (Nauka, Moscow), Vol. 1: The elements O, H, F, Cl, Br, I, He, Ne, Ar, Kr, Xe, Rn, S, N, P, and their compounds. (The volumes of this series are each in two separately bound parts: the text in Book 1, and tables of thermodynamic properties in Book 2.)

Glushko, V. P., Gurvich, L. V., Bergman, G. A., Veitz, I. V., Medvedev, V. A., Khachkuruzov, G. A., and Yungman, V. S. (**1979a**). *Thermodynamic Data for Individual Substances* (Nauka, Moscow), Vol. 2: The elements C, Si, Ge, Sn, and Pb and their compounds.

Glushko, V. P., Gurvich, L. V., Bergman, G. A., Veitz, I. V., Medvedev, V. A., Khachkuruzov, G. A., and Yungman, V. S. (**1981**). *Thermodynamic Data for Individual Substances* (Nauka, Moscow), Vol. 3: The elements B, Al, Ga, In, Tl, Be, Mg, Ca, Sr, and Ba and their compounds.

Glushko, V. P., Gurvich, L. V., Bergman, G. A., Veitz, I. V., Medvedev, V. A., Khachkuruzov, G. A., and Yungman, V. S. (**1983**). *Thermodynamic Data for Individual Substances* (Nauka, Moscow), Vol. 4: The elements Cr, Mo, W, V, Nb, Ta, Ti, Zr, Hf, Sc, Y, La, Th, U, Pu, Li, Na, K, Rb, Cs, and their compounds.

Glushko, V. P., Medvedev, V. A., Yungman, V. S., Bergman, G. A., Koselov, V. P., Gurvich, L. V., Vorob'yev', A. F., Kostryukov, V. P., Reznitskii, L. A., Ioffe, N. T. *et al.*, (**1979b**). *Thermodynamic Constants of Materials* (Natl. Acad. Sci. USSR, Institute for High Temperature, Moscow), Vol. IX: Be, Mg, Ca, Sr, Ba, Ra.

Grade, M., and Hirschwald, W. (**1982**). Ber. Bunsenges. Phys. Chem. **86**, 899.

Hilpert, K., and Gerads, H. (**1975**). High Temp. Sci. **7**, 11 (1975).

Hlavac, J. (**1982**). Pure Appl. Chem. **54**, 681.

Ho, P., and Burns, R. P. (1980). High Temp. Sci. **12**, 31.
Hultgren, R., Desai, P. D., Hawkins, D. T., Gleiser, M., Kelley, K. K., and Wagman, D. D. (1973). *Selected Values of the Thermodynamic Properties of the Elements* (American Society for Metals, Metals Park, OH).
Inghram, M. G., Chupka, W. A., and Porter, R. F. (1955). J. Chem. Phys. **23**, 2159.
Kelley, K. K. (1960). U.S. Bur. Mines Bull. **584**.
Kelley, K. K., and King, E. G. (1961). U.S. Bur. Mines Bull. **592**.
Kaufman, M., Wharton, L., and Klemperer, W. (1965). J. Chem. Phys. **43**, 943.
Kedrovskii, O. V., Kovtunenko, I. V., Kiseleva, E. V., and Bundel', A. A. (1967). Russ. J. Phys. Chem. **41**, 205.
Kazenas, E. K., Chizhikov, D. M., and Tsvetkov, Yu. V. (1968). Doklady Akad. Nauk SSSR **181**, 158.
Khanna, R. K., Stranz, D. D., and Donn, B. (1981). J. Chem. Phys. **74**, 2108.
Kudin, L. S., (1981). Izv. Vyssh. Uchebn. Zaved., Khim. Khim. Tekhnol. **24**, 837.
Lamoreaux, R. H., and Hildenbrand, D. L. (1984). J. Phys. Chem. Ref. Data **13**, 151.
Lau, K. H., and Hildenbrand, D. L. (1983). SRI International, Menlo Park, California, unpublished results.
Moore, C. E. (1949). "Atomic Energy Levels," Vol. 1, Natl. Bur. Stand. (U.S.) Circ. **467**.
Moore, C. E. (1952). "Atomic Energy Levels," Vol. 2, Natl. Bur. Stand. (U.S.) Circ. **467**.
Moore, C. E. (1958). "Atomic Energy Levels," Vol. 3, Natl. Bur. Stand. (U.S.) Circ. **467**.
Murad, E. (1981). J. Chem. Phys. **75**, 4080.
Newbury, R. S., Barton, Jr., G. W., and Searcy, A. W. (1968). J. Chem. Phys. **48**, 793.
Ogden, J. S., and Ricks, M. J. (1970). J. Chem. Phys. **52**, 352 (1970).
Olette, M., and Ancey-Moret, M. I. (1963). Rev. Metall. (Paris) **60**, 569.
Pankratz, L. B. (1982). *Thermodynamic Properties of Elements and Oxides*, U.S. Bureau of Mines Bull. 672.
Pedley, J. B., and Marshall, E. M. (1983). J. Phys. Chem. Ref. Data **12**, 967.
Porter, R. F., Chupka, W. A., and Inghram, M. G. (1955). J. Chem. Phys. **23**, 216.
Prochaska, E. S., and Andrews, L. (1980). J. Chem. Phys. **72**, 6782.
Richet, P., Bottinga, Y., Denielou, L., Petitet, J. P., and Tequi, C. (1982). Geochim. Cosmochim. Acta **46**, 2639.
Samsonov, G. V. *et al.* (1978). *Physicochemical Properties of Oxides: Handbook*, 2nd ed. (Metallurgiya, Moscow, USSR).
Schick, H. L. (1960). *Thermodynamics of Certain Refractory Compounds* (Academic, New York), Vols. 1 and 2.
Semenov, G. A., Popkov, O. S., Soloveichik, A. I., and Persiyaninova, S. N. (1972). Russ. J. Phys. Chem. **46**, 898.
Shunk, F. A. (1969). *Constitution of Binary Alloys* (McGraw–Hill, New York), Suppl. 2.
Stull, D. R. *et al.* (Eds.), *JANAF Thermochemical Tables*, 2nd ed. NSRDS-NBS 37 (U.S. GPO, Washington, DC, 1971). Individual table supplements to this reference are identified by the data of their issue. The published collections of supplementary tables are referenced separately. JANAF data not contained in the 1971 compendium or the collected supplements (Chase *et al.*, 1974, 1975, 1978, 1982) are referenced as dated supplements to the 1971 work.
Theard, L. P., and Hildenbrand, D. L. (1964). J. Chem. Phys. **41**, 3416.
Turkdogan, E. T. (1980). *Physical Chemistry of High Temperature Technology* (Academic, New York), pp. 230–234.
Vannerberg, N.-G. (1962). Prog. Inorg. Chem. **4**, 125.
Wagman, D. D., Evans, W. H., Parker, V. B., Schumm, R. H ., Halow, I., Bailey, S. M., Churney, K. L., and Nuttall, R. L. (1982). J. Phys. Chem. Ref. Data. **11**, Suppl. 2.
Wicks, C. E., and Block, F. E. (1963). U.S. Bur. Mines Bull. **605**.
Zmbov, K. F., Ames, L. L., and Margrave, J. L. (1973). High Temp. Sci. **5**, 235.